Neurobiology of Disease 203 (2024) 106726

Contents lists available at ScienceDirect

Neurobiology of Disease

journal homepage: www.elsevier.com/locate/ynbdi

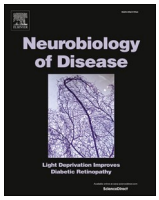

Early dysregulation of GSK3β impairs mitochondrial activity in Fragile X Syndrome

Giulia Cencelli [a], Giorgia Pedini [a], Carlotta Ricci [a], Eleonora Rosina [a], Giorgia Cecchetti [a], Antonietta Gentile [a], Giuseppe Aiello [b], Laura Pacini [a,c], Beatrice Garrone [d], Rosella Ombrato [d], Isabella Coletta [d], Federica Prati [d], Claudio Milanese [d], Claudia Bagni [a,b,*]

[a] Department of Biomedicine and Prevention, University of Rome Tor Vergata, 00133 Rome, Italy
[b] Department of Fundamental Neurosciences, University of Lausanne, 1005 Lausanne, Switzerland
[c] Faculty of Medicine, UniCamillus, Saint Camillus International University of Health and Medical Sciences, 00131 Rome, Italy
[d] Angelini Pharma S.p.A., 00181 Rome, Italy

ARTICLE INFO

Keywords:
Autism
Peroxisome Proliferator-Activated Receptor Gamma
Coactivator (PGC) 1-alpha
GSK3β-inhibitor
Intellectual disabilities

ABSTRACT

The finely tuned regulation of mitochondria activity is essential for proper brain development. Fragile X Syndrome (FXS), the leading cause of inherited intellectual disability, is a neurodevelopmental disorder in which mitochondrial dysfunction has been increasingly implicated. This study investigates the role of Glycogen Synthase Kinase 3β (GSK3β) in FXS. Several studies have reported the dysregulation of GSK3β in FXS, and its role in mitochondrial function is also well established. However, the link between disrupted GSK3β activity and mitochondrial dysfunction in FXS remains unexplored. Utilizing *Fmr1* knockout (KO) mice and human cell lines from individuals with FXS, we uncovered a developmental window where dysregulated GSK3β activity disrupts mitochondrial function. Notably, a partial inhibition of GSK3β activity in FXS fibroblasts from young individuals rescues the observed mitochondrial defects, suggesting that targeting GSK3β in the early stages may offer therapeutic benefits for this condition.

1. Introduction

Mitochondria are double-membrane organelles essential for energy production through the generation of adenosine triphosphate (ATP). Neurons rely heavily on proper mitochondrial function to maintain their activity and support critical processes like neurotransmitter release and synaptic development (Belenguer et al., 2019; Duarte et al., 2023; Faria-Pereira and Morais, 2022; Ozgen et al., 2022; Pekkurnaz and Wang, 2022; Trigo et al., 2022; Ülgen et al., 2023). In fact, mitochondrial dysfunction has emerged as a contributing factor in various neurological conditions, including Fragile X Syndrome (FXS) and autism spectrum disorder (ASD) (Anitha et al., 2023; Cabral-Costa and Kowaltowski, 2020; Clemente-Suárez et al., 2023; Hollis et al., 2017; Kanellopoulos et al., 2020; Valenti and Vacca, 2023).

FXS represents the most prevalent form of monogenic hereditary intellectual disability (ID) and autism. FXS arises from a dynamic mutation in the *FMR1* gene, encoding the RNA-binding protein Fragile X Messenger Ribonucleoprotein (FMRP), crucial for proper brain function and development (Bagni and Zukin, 2019; Richter and Zhao, 2021). Individuals with FXS are characterized by cognitive impairments and behavioral abnormalities, which are frequently linked to intellectual disability and ASD (Acero-Garcés et al., 2023; Elhawary et al., 2023; Hagerman et al., 2017; Protic and Hagerman, 2024). FXS is also associated with changes in mitochondria function. These changes, which include altered levels of mitochondrial proteins, mitochondrial fragmentation, and abnormal mitochondrial activity, are thought to significantly affect neuronal function in FXS (Bülow et al., 2021a, 2021b; D'Antoni et al., 2020; Geng et al., 2023; Grandi et al., 2024; Griffiths et al., 2020; Licznerski et al., 2020; Mithal and Chandel, 2020; Nobile et al., 2020; Shen et al., 2023; Shen et al., 2019).

One of the signaling pathways involved in the regulation of mitochondrial biogenesis and activity is the Glycogen Synthase Kinase 3β (GSK3β) signaling pathway (Wang et al., 2022). GSK3 is a constitutively active serine/threonine kinase, existing as two isoforms, GSK3α and GSK3β. The β isoform is highly expressed in the central nervous system (CNS) and its activity is negatively regulated by inhibitory

* Corresponding author at: Department of Fundamental Neurosciences, University of Lausanne, 1005 Lausanne, Switzerland
E-mail address: claudia.bagni@unil.ch (C. Bagni).

https://doi.org/10.1016/j.nbd.2024.106726
Received 7 June 2024; Received in revised form 3 November 2024; Accepted 3 November 2024
Available online 5 November 2024

phosphorylation at serine 9 (Beurel et al., 2015). While both isoforms contribute to different cellular functions, GSK3β has been specifically implicated in regulating mitochondrial biogenesis and activity (Martin et al., 2018; Yang et al., 2017). At the level of mitochondria, GSK3β acts primarily on the Peroxisome Proliferator-Activated Receptor Gamma, Coactivator 1-alpha (PGC1α), a co-transcriptional factor that controls the expression of several genes involved in energy metabolism (Anderson et al., 2008; Martin et al., 2018; Rippin and Eldar-Finkelman, 2021; Souder and Anderson, 2019; Souder et al., 2023; Theeuwes et al., 2020; Xu et al., 2014; Yang et al., 2017). Noteworthy, a dysregulation of GSK3β activity has been reported in the *Fmr1* knockout (KO) mouse model of FXS (Franklin et al., 2014; Min et al., 2009; Yuskaitis et al., 2010), contributing to some FXS-associated behavioral defects (D'Incal et al., 2022; Marosi et al., 2022; Rizk et al., 2021). Interestingly, in FXS mice, the administration of GSK3β inhibitors, such as lithium, ameliorates impaired behaviors like social anxiety, susceptibility to seizures, hyperactivity, and cognitive alterations including hippocampus-dependent learning and trace fear memory (reviewed in Rizk et al., 2021). Nevertheless, the inhibition of GSK3β as potential treatment in individuals with FXS remains largely unexplored, despite the promising indication in a pilot clinical trial with lithium (Berry-Kravis et al., 2008).

Although GSK3β dysregulation has been reported in FXS, its link to mitochondrial dysfunction/s in FXS remains largely unexplored. Additionally, a knowledge gap remains on the developmental dynamics of GSK3β in FXS. Since the brain undergoes critical periods of development (Cisneros-Franco et al., 2020; Dehorter and Del Pino, 2020), where precise protein expression is important for its optimal function (Bagni and Zukin, 2019; Gonzalez-Lozano et al., 2016; van Oostrum et al., 2023; Sala and Segal, 2014), elucidating the changes in GSK3β activity and expression during development is essential to understand some of the mechanisms underlying FXS and to identify a critical window for targeted therapeutic intervention. Therefore, the aim of this work was to address when the previously described dysregulation of GSK3β in FXS occurs and to elucidate its possible link to the reported mitochondrial alterations. Our findings reveal an age-dependent dysregulation of GSK3β activity in both FXS mice and human cells. Notably, the early stages of development appear to be a critical window where GSK3β disruption leads to impaired mitochondrial function. Finally, we demonstrate that the treatment of FXS fibroblasts with the ATP-competitive GSK3 inhibitor AFC05976 (Buonfiglio et al., 2020; Prati et al., 2020) restored mitochondrial defects.

2. Materials and methods

2.1. Animals

Fmr1 KO (Bakker et al., 1994) (FVB·129P2(B6)) and WT mice (FVB·129P2(B6)) were bred and maintained in-house in a homozygous state. Food and water were provided *ad libitum* and light-dark phases lasted 12 h (from 7 a.m. to 7 p.m.). Animal housing and care were carried out according to institutional guidelines in compliance with international laws and policies (European Community Guidelines for Animal Care, DL 116/92, application of the European Communities Council Directive, 86/609/EEC). Studies were approved by the Institutional Ethical Board at the University of Rome Tor Vergata, according to the guideline of the Italian Institute of Health (protocol n. 1138/2016-PR and 745/2022-PR).

2.2. Synaptoneurosome preparation

Synaptoneurosomes were prepared by homogenization of fresh cortical, and hippocampal tissues in ice-cold buffer as previously described (Mercaldo et al., 2023). In brief, tissues from male *Fmr1* KO and WT mice at different developmental stages (post-natal day 7 (P7) - P14 and P120) were homogenized in ice-cold 0.32 M sucrose solution containing 1 mM EDTA, 1 mg/ml bovine serum albumin, and 5 mM HEPES pH 7.4, in a Potter-Elvehjem homogenizer with a Teflon piston (10 up-and-down strokes) on ice. The suspension was centrifuged at 3,000 x*g* for 8 min at 4 °C, and the supernatant clarified for an additional 4 min at 3,000 x*g* at 4 °C. The supernatant was collected and centrifuged at 14,000 x*g* for 12 min at 4 °C. The pellet was resuspended in 1 ml of a 45 % (vol/vol) Percoll solution in a Krebs-Ringer solution (144 mM NaCl, 5 mM KCl, 10 mM HEPES, 1 mM EDTA, and 5 mM glucose, pH 7.4). After centrifugation at 14,000 x*g* for 4 min, the top layer was removed (synaptoneurosomal fraction) and washed in 1 ml of Krebs-Ringer solution. The synaptoneurosomes were snap-frozen in liquid nitrogen for further analysis.

2.3. Western blot

Standard methodologies were used. Protein extracts from synaptoneurosome purifications and cell lysates were separated by 10 % or 8 % SDS-PAGE and transferred to a PVDF membrane. Membranes were incubated using the following specific primary antibodies: rabbit anti-GSK3β (1:1000, Cell Signaling Technology), rabbit anti-phospho-GSK3β (S9) (1:1000, Cell Signaling Technology), mouse anti-β-actin (ACTB) (1:5000, Merck), rabbit anti-phospho-GSK3α (S21) (1:500, Cell Signaling Technology), rabbit anti-GSK3α (1:1000, Cell Signaling Technology), mouse anti-β-catenin (1:2000, Invitrogen, Thermo Fisher Scientific), mouse anti-PGC1α (1:1000, Merck), mouse anti-Vinculin (1:2000, Merck), mouse anti-PSD95 (1:2000 Invitrogen, Thermo Fisher Scientific), mouse anti-Synaptophysin (1:2000, Abcam) and rabbit anti-FMRP (1:1000, produced in house PZ1 (Pedini et al., 2022)). The following secondary antibodies were used: HRP-conjugated anti-rabbit or anti-mouse secondary antibodies (1:5000, Cell Signaling Technology). Proteins were revealed using an enhanced chemiluminescence kit (Bio-Rad) and the imaging system LAS-4000 mini (GE Healthcare). Total and phospho-protein levels were detected on the same membranes. Membranes were first probed with an antibody specific for phospho-GSK3β (S9) or phospho-GSK3α (S21) and next stripped using a stripping solution (Restore™ PLUS Western Blot Stripping Buffer, Thermo Fisher Scientific) to remove the phosphorylated signal according to manufacturer's instructions. After each stripping, the absence of signal was confirmed before incubating the membrane with the total rabbit anti-GSK3β or anti-GSK3α antibodies (1:1000, Cell Signaling Technology), enabling direct comparison of phosphorylated and total GSK3α or β levels within each sample. Specifically, phospho-GSK3β (S9) or phospho-GSK3α (S21) were normalized relative to the total GSK3β or GSK3α, respectively, on the same blot. Quantification was performed using the IQ ImageQuant TL software (GE Healthcare). Total protein levels were normalized to the average of Vinculin or ACTB and Coomassie blue staining. For all SDS-PAGE PageRuler™ Plus Prestained Protein Ladder (10 to 250 kDa, Thermo Fisher Scientific) was used.

2.4. Mitochondrial functional assays

A total of 50 μg of synaptoneurosomes were resuspended in Mitochondrial Respiration Medium (MiR05) buffer (according to Oroboros Instruments' instructions). The synaptoneurosome suspension was loaded into an Oroboros Oxygraph-2K (O2k) chamber and the oxygen consumption rates were measured before and after the addition of the following substrates and specific inhibitors: 1) 10 μg/ml digitonin (Merck), 1 mM malate (Merck), 2.5 mM pyruvate (Merck), 10 mM glutamate (Merck), followed by 2.5 mM ADP (Calbiochem) to determine complex I-driven oxidative phosphorylation (CI OXPHOS); 2) 5 mM succinate (Merck) to determine the oxidative phosphorylation driven by simultaneous activation of complex I and II (CI + II OXPHOS); 3) 0.2 mM carbonyl cyanide *m*-chlorophenyl hydrazone (CCCP) (Sigma-Aldrich, Merck) to reach the maximal, uncoupled respiration (CI + II electron transfer system, ETS); 4) 0.5 μM rotenone (Merck) to fully inhibit complex I-driven respiration and measure complex II-driven uncoupled

respiration (CII electron transfer system, CII ETS); 5) 0.5 μM antimycin A (Merck) to block mitochondrial respiration at the level of complex III; 6) 2 mM sodium ascorbate (Merck), 0.5 mM *N,N,N′,N′*-tetramethyl-*p*-phenylenediamine dihydrochloride (TMPD; Merck) and 100 mM sodium azide (Merck) to measure cytochrome *c* oxidase (CIV or COX)-driven respiration.

2.5. Cultures of human fibroblasts, induced pluripotent stem cells (iPSCs) and neural differentiation

Control fibroblast cell lines (males, $n = 11$, age range 6–43 years) were purchased from the Coriell Cell Repositories. FXS fibroblast cell lines (males, $n = 14$, age range 4–37 years) were obtained from dermal biopsies with patient consent and under the approval from multiple centers (CHUV University Hospital of Lausanne; M.I.N.D. Institute in Sacramento; Erasmus Medical Center in Rotterdam). Investigations were carried out following the rules of the Declaration of Helsinki of 1975 revised in 2013. The approval from the Institutional Review Board (IRB) was obtained before undertaking the research to confirm that the study meets national and international guidelines. Our study is based on previously characterized human cell lines (Cencelli et al., 2023; Jacquemont et al., 2018), under the approval of the ethics committee of the University Hospital of Lausanne (Switzerland), review board of the University of California Davis Medical Center (USA), review board of the Erasmus Medical Center of Rotterdam (The Netherlands). The clinical assessment, inclusion criteria, study protocol, *FMR1* mRNA and FMRP levels, and all amendments have been previously described (Cencelli et al., 2023; Jacquemont et al., 2018). One additional FXS cell line purchased from the Coriell Cell Repositories was included in this study (GM05848).

Fibroblasts were maintained in DMEM/F-12 (Gibco, Thermo Fisher Scientific) supplemented with 10 % fetal bovine serum (Gibco, Thermo Fisher Scientific), 1× GlutaMax™ (Gibco, Thermo Fisher Scientific), 1× penicillin-streptomycin (Gibco, Thermo Fisher Scientific) and MycoZap reagent (Lonza).

Induced pluripotent stem cells (iPSCs) derived from fibroblasts of typically developing individuals (TDI) and FXS individuals were established at the Children's Hospital of Orange County and kindly provided by Dr. Philip H. Schwartz (Brick et al., 2014). iPSCs were cultured on Matrigel (BD Biosciences) in mTeSR medium (Stem Cell Technologies). The clinical characteristics of iPSCs used in the present study and the relative *FMR1* mRNA and FMRP levels have been previously described (Cencelli et al., 2023). iPSCs were differentiated into neurons as previously described (Cencelli et al., 2023; Espuny-Camacho et al., 2013). Briefly, iPSCs were maintained in culture in defined default media (DDM) consisting of DMEM/F-12 supplemented with 1× N-2 supplement (Gibco, Thermo Fisher Scientific), 1× B-27 supplement (Gibco, Thermo Fisher Scientific), bovine albumin fraction V 7.5 % (Gibco, Thermo Fisher Scientific), 1× MEM non-essential amino acids (Gibco, Thermo Fisher Scientific), 1 mM sodium pyruvate (Gibco, Thermo Fisher Scientific), 100 μM β-mercaptoethanol (Gibco, Thermo Fisher Scientific), and 100 ng/ml human recombinant Noggin (Stem Cell Technologies) with a daily medium change. After 16 days, the medium was changed to DDM, supplemented with B-27 supplement (Gibco, Thermo Fisher Scientific) without recombinant Noggin. After 24 days, cells were dissociated and plated into poly-ornithine/laminin-coated wells. Five to seven days after dissociation, half of the medium was replaced with neurobasal (Gibco, Thermo Fisher Scientific) supplemented with 1× B-27 supplement (Gibco, Thermo Fisher Scientific) and 2 mM glutamine (Gibco, Thermo Fisher Scientific).

2.6. GSK3 inhibitor treatment

Fibroblasts were treated with increasing concentrations of the GSK3 inhibitor AFC05976 (Buonfiglio et al., 2020; Prati et al., 2020) (0.003, 0.01, 0.03, 0.1, 0.3 μM; Angelini Pharma S.p.A., Rome, Italy), dissolved in dimethyl sulfoxide (DMSO). After a 24-h incubation, the cells were used for molecular studies (protein and RNA analysis) and mitochondrial activity assessment.

2.7. RT-qPCR

Total RNA was extracted with TRIzol according to the manufacturer's protocol (Invitrogen, Thermo Fischer Scientific). For the synthesis of cDNA, 500 ng of RNA were retrotranscribed using 200 U/ml M-MLV Reverse Transcriptase (Invitrogen, Thermo Fisher Scientific). mRNAs were quantified by real-time PCR using SYBR® Green Master Mix (Bio-Rad) on StepOnePlus™Real-Time PCR machine (Applied Biosystems, Thermo Fischer Scientific) according to the manufacturer's instructions using specific primers. mRNA levels were expressed as relative abundance compared to *mActb* or *hHPRT1* mRNAs using the (2^{-DDCT}) method. The primers used for the amplification of the selected nuclear-encoded mitochondrial genes are:

mCox5b Forward 5′ – GGGCTGCATCTGTGAAGAGGACA – 3′
mCox5b Reverse 5′ – GGGGCATCGCTGACTCTCGC – 3′
mNdufb4 Forward 5′ – CCTTGATTCGCTGGACCTAT – 3′
mNdufb4 Reverse 5′ – CCTGCCACAGCTCCTAAAAG – 3′
mCox5a Forward 5′ – TTGATGCCTGGGAATTGCGT – 3′
mCox5a Reverse 5′ – TTAACCGTCTACATGCTCGC – 3′
mUqcrc2 Forward 5′ – GCTAGAGCCATGAAGCTCCTC – 3′
mUqcrc2 Reverse 5′ – CTTCGGGGCAACTTTGAGGG – 3′
mAtp5g2 Forward 5′ – GAGCACCTCTCAGCTGCTGAGTCG – 3′ (Licznerski et al., 2020)
mAtp5g2 Reverse 5′ – GGCCTCTGAGAGGGCAAAGCC – 3′ (Licznerski et al., 2020)
mActb Forward 5′ – CGTCCACCCGCGAGCACA – 3′
mActb Reverse 5′ – TCCATGGCGAACTGGTGGC – 3′
mAtp5b Forward 5′ – CCACCACCAAGAAGGGATCG – 3′
mAtp5b Reverse 5′ – TCCAAATGGGCAAAGGTGGT – 3′
hCOX5B Forward 5′ – TTACTTCGCGGAGCTGGAAC – 3′
hCOX5B Reverse 5′ – TCATCAGTGGGAACACCACC – 3′
hNDUFB4 Forward 5′ – GCCATAAGAGCCCAGCTGAA – 3′
hNDUFB4 Reverse 5′ – TCTTGCATAGGCCCAACGAA – 3′
hCOX5A Forward 5′ – AGATGCCTGGGAATTGCGTA – 3′
hCOX5A Reverse 5′ – CATTTAACCGTCTGCATGCCC – 3′
hUQCRC2 Forward 5′ – TTTAATCCGGCAGTGACCGT – 3′
hUQCRC2 Reverse 5′ – GGGGGCAACTTTGAGGGAAT – 3′
hATP5G2 Forward 5′ – CCGGATACCGCCACAGC – 3′
hATP5G2 Reverse 5′ – GCGAACATTTTCAGGGGGTG – 3′
hHPRT1 Forward 5′ – TGCTGAGGATTTGGAAAGGGT – 3′
hHPRT1 Reverse 5′ – TCGAGCAAGACGTTCAGTCC – 3′

2.8. ATP measurement

ATP levels were quantified using an ATP assay kit (Abcam) following the manufacturer's protocol. Briefly, synaptoneurosomes or fibroblasts were lysed in the provided buffer and deproteinized using a Deproteinizing Sample Preparation Kit – TCA (Abcam). ATP levels were then measured by fluorescence at an excitation/emission wavelength of 535/587 nm.

2.9. Mitochondrial membrane potential - TMRE assay and imaging

The mitochondrial membrane potential was measured using tetramethylrhodamine ethyl ester perchlorate (TMRE) (Enzo Life Sciences). Human fibroblasts were incubated for 30 min at 37 °C with 10 nM TMRE in DMEM/F-12 (Gibco, Thermo Fisher Scientific) supplemented with 10 % fetal bovine serum (Gibco, Thermo Fisher Scientific), 1× GlutaMax™ (Gibco, Thermo Fisher Scientific), 1× penicillin-streptomycin (Gibco, Thermo Fisher Scientific) and MycoZap reagent (Lonza). After incubation, fibroblasts were imaged on a Leica CTR6000 microscope using HC PL APO 63×/1.40 oil CS2 objective. To quantify fluorescence intensity,

ImageJ software was used. Each cell was segmented using a threshold-based mask function within ImageJ, ensuring consistent segmentation across all images. The mean gray value (fluorescent intensity per pixel) of each mask was then measured to quantify the average fluorescence intensity within each cell.

2.10. Oxygen consumption - seahorse assay

The mitochondrial activity and specifically the oxygen consumption was measured using the Seahorse XFp analyzer (Agilent Technologies). Fibroblasts were seeded at a density of 15,000 cells per well in an eight-well miniplate format. After 48 h, the culture medium was replaced with fresh XF Base Medium (Agilent Technologies) supplemented with 10 mM glucose, 1 mM sodium pyruvate (Gibco, Thermo Fisher Scientific), and 2 mM L-glutamine (Gibco, Thermo Fisher Scientific) according to the manufacturer's instructions. Following a one-hour incubation at 37 °C in a non-CO_2 incubator, the oxygen consumption rate (OCR) was measured. Oligomycin (1.5 μM), carbonyl cyanide-*p*-trifluoromethoxyphenylhydrazone (FCCP, 2 μM), and a combination of rotenone (0.5 μM) and antimycin A (0.5 μM) were pre-loaded into the injection ports of a hydrated sensor cartridge. These compounds were sequentially injected into the wells during the assay. The OCR measurements were then normalized to cell number. Mitochondrial respiratory function was assessed by calculating specific parameters from the OCR profile. Basal respiration was defined as the OCR rate before oligomycin injection. ATP-linked respiration, representing mitochondrial

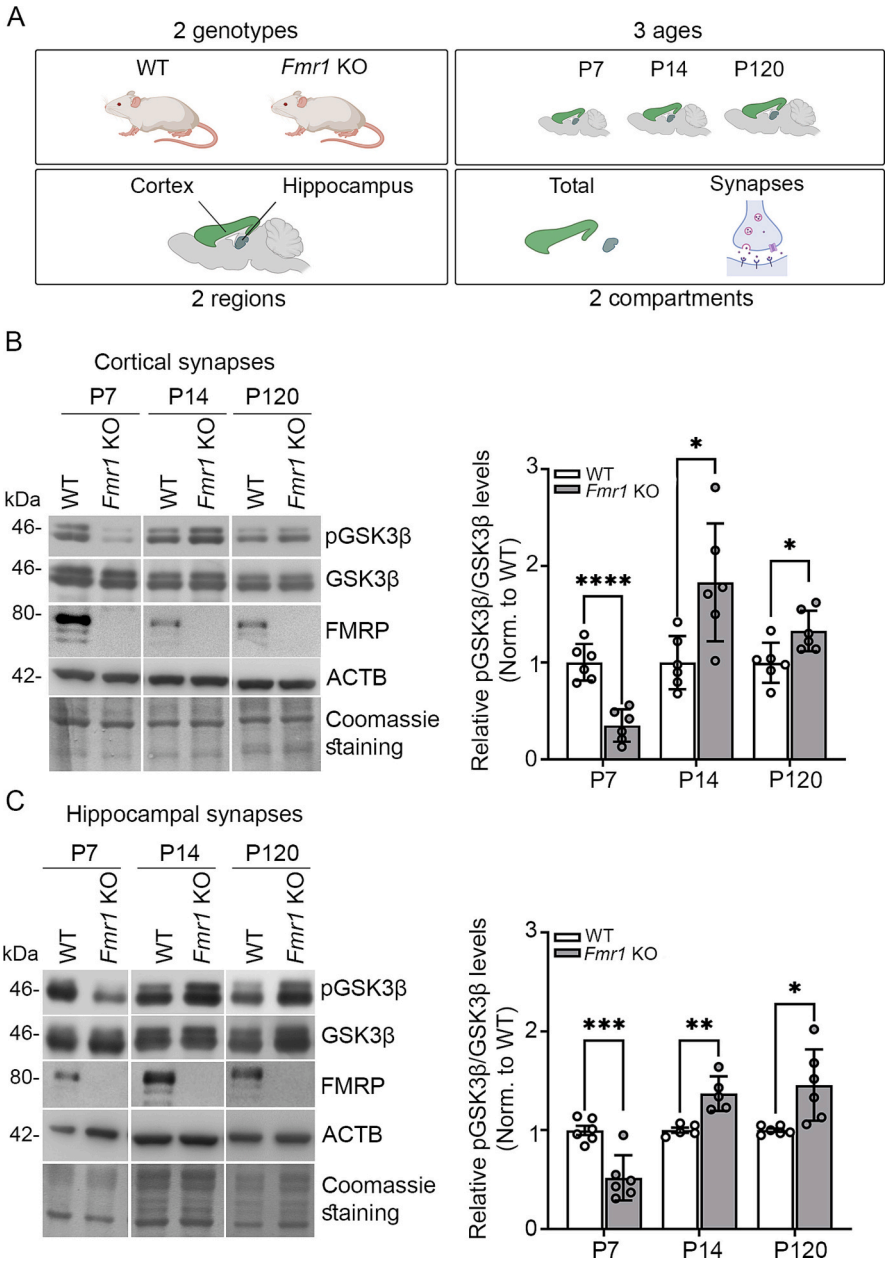

Fig. 1. GSK3β activity at synapses in WT and *Fmr1* KO mice. (A) Scheme of the experimental design in mice. Two different genotypes (WT and *Fmr1* KO), two brain regions (cortex and hippocampus), total (all cells) and synaptoneurosome extracts were isolated at three different developmental stages (P7, P14 and P120) (image created in BioRender.com). (B—C) Representative Western blots showing pGSK3β (S9), GSK3β, and FMRP levels in WT and *Fmr1* KO mice at different developmental stages in (B) cortical and (C) hippocampal synapses. The bar plots represent the quantification of pGSK3β(S9)/GSK3β in WT and *Fmr1* KO mice. β-actin (ACTB) and Coomassie staining were used as loading controls. Error bars represent the SD (**** $p < 0.0001$, *** $p < 0.001$, ** $p < 0.01$, * $p < 0.05$, Multiple Student's *t*-test) ($n =$ 5–6 per genotype).

oxygen consumption for ATP production, was calculated as the difference between basal OCR and oligomycin-induced OCR. Maximal respiration, reflecting the maximum capacity of the electron transport chain, was determined as the difference between FCCP-stimulated OCR and the rate measured after rotenone/antimycin A injection.

2.11. Statistics

Statistical analysis was performed with Prism GraphPad 9. The significance level was established at $p < 0.05$. Differences between two groups were analyzed using unpaired Student's *t*-test. One-way ANOVA, followed by Dunnett's multiple comparisons test was used for the analysis of the dose-response experiments with the AFC05976 inhibitor. Two-way ANOVA without repeated measures, followed by Sidak's multiple comparisons test, was performed to examine the effect of genotype and treatment and their interaction. All data are expressed as fold change relative to WT animals or TDI as mean ± SD.

3. Results

3.1. Synaptic activity of GSK3β in Fmr1 KO mice is dysregulated during development

GSK3β regulates different neuronal processes, including dendritic spine formation, synapse development and plasticity and maintenance of synaptic structure (Banach et al., 2022; Jaworski et al., 2019; Kondratiuk et al., 2017; Ochs et al., 2015; Wang et al., 2019; Xing et al., 2016). Therefore, potential alterations of GSK3β were investigated at synapses (Fig. 1A). Since the behavioral improvements previously observed with GSK3β inhibition likely involve restored function in brain regions critical for learning and memory (Rizk et al., 2021), such as the cortex and the hippocampus, our investigation largely focused on these two brain areas.

At first, the level and the activity of GSK3β were evaluated by assessing the phosphorylation status of serine 9 (pGSK3β S9) in the *Fmr1* KO. Such a modification leads to the inactivation of enzymatic activity (Beurel et al., 2015). Total GSK3β levels and its phosphorylated form (pGSK3β S9) were analyzed in total and synaptic protein extracts from cortex and hippocampus at three distinct developmental stages: early postnatal (P7), late postnatal (P14), and adult (P120) (Fig. 1A). The purity of the synaptoneurosomal preparations was confirmed by assessing the enrichment of specific markers for postsynaptic and presynaptic components, PSD95 and synaptophysin, respectively (Fig. S1A). Our findings revealed an increase of GSK3β activity in cortical and hippocampal synapses in *Fmr1* KO mice at P7. In contrast, starting from P14, GSK3β activity switched to hypoactivation in the same regions (Fig. 1B-C), whereas no significant differences were observed at synapses in the expression of total GSK3β (Fig. S1B) and in pGSK3β (S9) in total extracts (Fig. S1C-D). Our data indicate a specific impact of GSK3β activity specifically at FXS synapses during brain development, as the GSK3α activity did not change across different ages between WT and *Fmr1* KO (Fig. S2).

3.2. The expression of PGC1α-regulated mitochondrial genes is altered in Fmr1 KO mice

To investigate whether a dysregulated GSK3β activity affects mitochondria, we first monitored the expression of PGC1α, a master regulator of mitochondrial biogenesis and function. As illustrated in Fig. 2A, GSK3β-mediated phosphorylation of PGC1α promotes its degradation, also leading to decreased expression of mitochondrial related genes (Anderson et al., 2008; Chen et al., 2022; Souder and Anderson, 2019; Theeuwes et al., 2020; Wang et al., 2022). PGC1α levels decrease in cortical and hippocampal *Fmr1* KO synapses at P7 (Fig. 2B), consistent with the observed GSK3β hyperactivity. To further investigate the impact of altered GSK3β-PGC1α axis on mitochondrial function, we focused on a specific set of nuclear-encoded mitochondrial genes, previously reported to be deregulated in neurological or mitochondrial disorders (Anitha et al., 2013; Ch'ng et al., 2015; Föcking et al., 2016; Licznerski et al., 2020; Toomey et al., 2022) and identified as responsive to PGC1α alteration or GSK3β inhibition (Martin et al., 2018; Scarpulla, 2011; Souder et al., 2023). We observed reduced levels of mRNAs encoding for the Membrane Subunit c of the Mitochondrial ATP Synthase (*Atp5g2*) (complex V), ATP Synthase F1 Subunit Beta (*Atp5b*) (complex V), the Cytochrome C Oxidase Subunit 5 A and 5 B (*Cox5a*, *Cox5b*) (complex IV), the NADH:Ubiquinone Oxidoreductase Subunit B4 (*Ndufb4*) (complex I), and the Ubiquinol-Cytochrome C Reductase Core Protein 2 (*Uqcrc2*) (complex III) in cortical and hippocampal synapses of P7 *Fmr1* KO mice compared to WT animals (Fig. 2C). On the other hand, adult *Fmr1* KO mice, where the activity of GSK3β is reduced, showed increased levels of PGC1α (Fig. 2 D-E) and a consequent increase of *Atp5g2, Cox5b* and *Ndufb4* mRNA levels in both cortical and hippocampal synapses (Fig. 2F).

To assess whether the observed downregulation of mitochondrial gene expression translates to impaired mitochondrial function in FXS, ATP levels were measured in cortical and hippocampal synapses isolated from P7 and P120 WT and *Fmr1* KO mice (Fig. 2G-H). Notably, FXS mice at P7 displayed a significant reduction in ATP levels compared to WT (Fig. 2G), while no significant differences were observed in P120 mice (Fig. 2H). Finally, we independently assessed mitochondrial activity also in hippocampal synaptoneurosomes from P7 mice using high-resolution respirometry using the Oroboros O2k system. A significant decrease of the complex II electron transport system (CII ETS) activity was observed in the *Fmr1* KO hippocampal synaptoneurosomes compared to WT, corroborating a mitochondrial dysfunction at FXS synapses (Fig. S3). Overall, these results suggest that dysregulated GSK3β activity may contribute to mitochondrial defects in FXS, in a developmental-dependent manner.

3.3. GSK3β dysregulation impairs mitochondrial activity in FXS fibroblasts

To assess whether GSK3β dysregulation observed in the FXS mouse model translates to humans, GSK3β expression and activity were analyzed in human fibroblasts derived from TDI ($n = 11$) and individuals with FXS ($n = 14$), grouped according to the age (Fig. 3A). GSK3β activity increased (less pGSK3β) in the youngest group of FXS individuals (group 1; age < 10 year-old; TDI $n = 3$; FXS $n = 3$; Fig. 3B). In contrast, group 2 (age between 10 and 20 year-old; TDI $n = 5$; FXS $n = 6$) showed reduced GSK3β activity, mirrored by an increased expression of pGSK3β (S9) (Fig. 3B). No differences of GSK3β activity were reported in adult individuals (group 3, age > 20 year-old; TDI $n = 3$; FXS $n = 5$) (Fig. 3B), nor in the total levels of GSK3β (Fig. S4A). Of note, these results partially recapitulate the findings observed in the murine model (Fig. 1). We next explored GSK3β activity in iPSC-derived neurons and did not find significant differences of pGSK3β between TDI and FXS (Fig. S4B), consistent with our findings showing postnatal dysregulation of GSK3β activity in *Fmr1* KO mice. Of note, iPSC-derived neurons may not fully represent the full maturity of neuronal cells, as previously suggested (Espuny-Camacho et al., 2013).

To further investigate the relationship between GSK3β deregulation and mitochondria, PGC1α and mitochondrial gene expression were examined in human fibroblasts (Fig. 3C-E). PGC1α levels (Fig. 3D) and the expression of some mitochondrial genes (*ATP5G2*, *COX5B*, *NDUFB4*, and *UQCRC2*; Fig. 3E) were downregulated in young FXS fibroblasts compared to TDI, while *COX5A* shows a trend towards a decreased expression. The overall pattern of mitochondrial gene expression therefore mirrored the observed defects in the murine model. To investigate whether dysregulated mitochondrial gene expression might affect the function of mitochondria in FXS fibroblasts, oxygen consumption rate (OCR) was measured using the Seahorse XFp Analyzer. Fibroblasts derived from young FXS individuals exhibited a reduction in

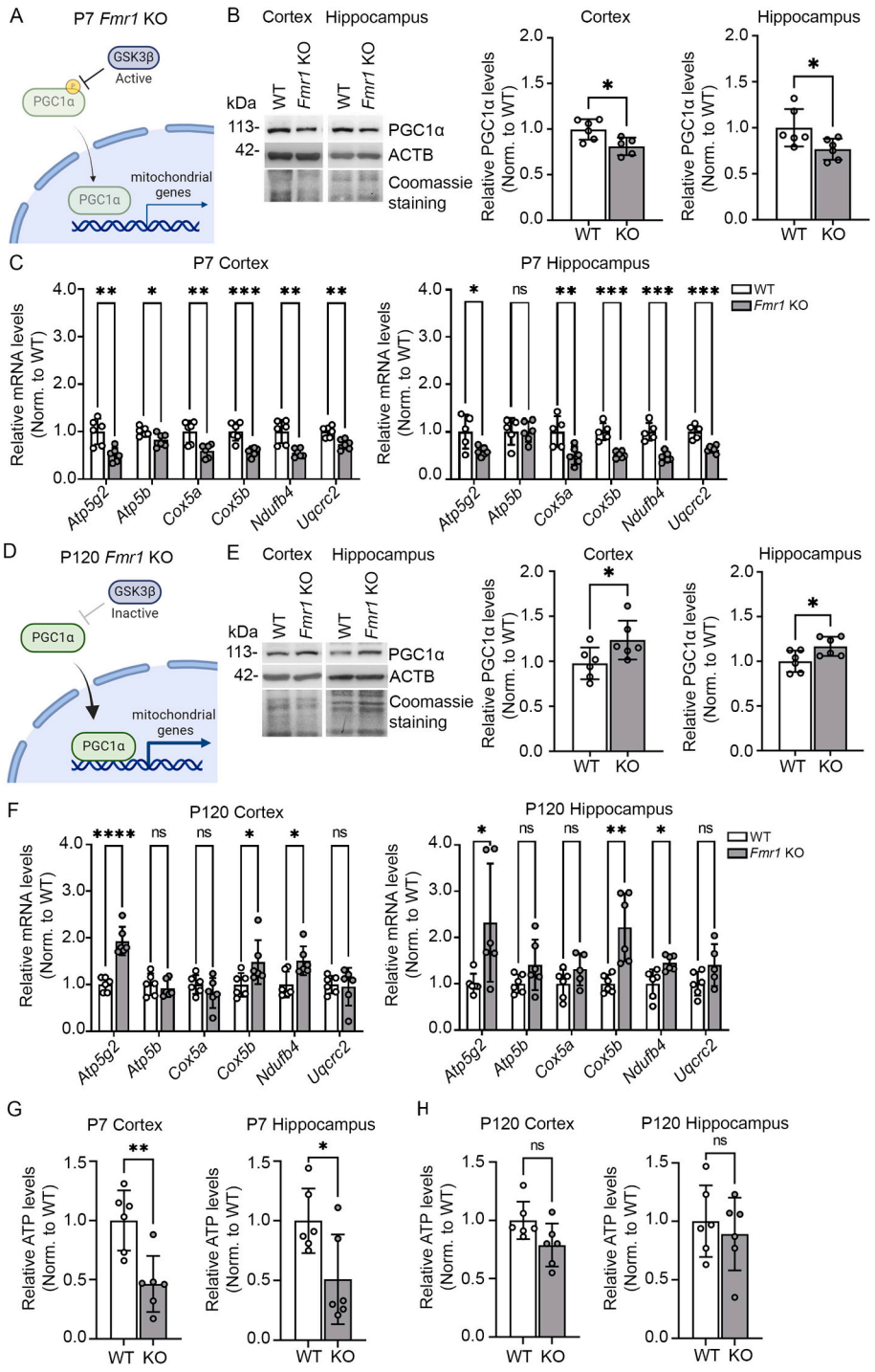

Fig. 2. PGC1α-regulated mitochondrial genes and synaptic activity in WT and *Fmr1* KO mice. (A) Schematic representation of GSK3β - PGC1α pathway in P7 *Fmr1* KO animals (image created in BioRender.com). (B) Left, representative Western blots showing PGC1α levels in cortical and hippocampal synapses from P7 WT and *Fmr1* KO mice. Right, the bar plots represent the quantification of PGC1α levels. β-actin (ACTB) and Coomassie staining were used as loading controls. Error bars represent the SD (* $p < 0.05$, Student's *t*-test) (n = 5-6 per genotype). (C) The bar plots show the quantification of *Atp5g2*, *Atp5b, Cox5a, Cox5b*, *Ndfub4,* and *Uqcrc2* mRNA levels in young (P7) WT and *Fmr1* KO mice in cortical and hippocampal synapses, normalized to *Actb* mRNA levels. Error bars represent the SD (*** $p < 0.001$, ** $p < 0.01$, * $p < 0.05$, ns = non-significant, Multiple Student's *t*-test) (n = 5–6 per genotype). (D) Schematic representation of GSK3β - PGC1α pathway in P120 *Fmr1* KO animals (image created in BioRender.com). (E) Left, representative Western blots showing PGC1α levels in P120 WT and *Fmr1* KO mice in cortical and hippocampal synapses. Right, the bar plots represent the quantification of PGC1α levels. β-actin (ACTB) and Coomassie staining were used as loading controls. Error bars represent the SD (* $p < 0.05$, Student's *t*-test) (n = 6 per genotype). (F) The bar plots show the quantification of *Atp5g2*, *Atp5b, Cox5a, Cox5b*, *Ndfub4,* and *Uqcrc2* mRNA levels in adult (P120) WT and *Fmr1* KO mice in cortical and hippocampal synapses, normalized to *Actb* mRNA levels. Error bars represent the SD (**** $p < 0.0001$, ** $p < 0.01$ * $p < 0.05$, ns = non-significant, Multiple Student's *t*-test) (n = 5–6 per genotype). (G-H) The bar plots show the quantification of ATP levels in P7 (G) and P120 (H) WT and *Fmr1* KO mice in cortical and hippocampal synapses. Error bars represent the SD (** $p < 0.01$, * $p < 0.05$, ns = non-significant, Student's *t*-test) (n = 6 per genotype).

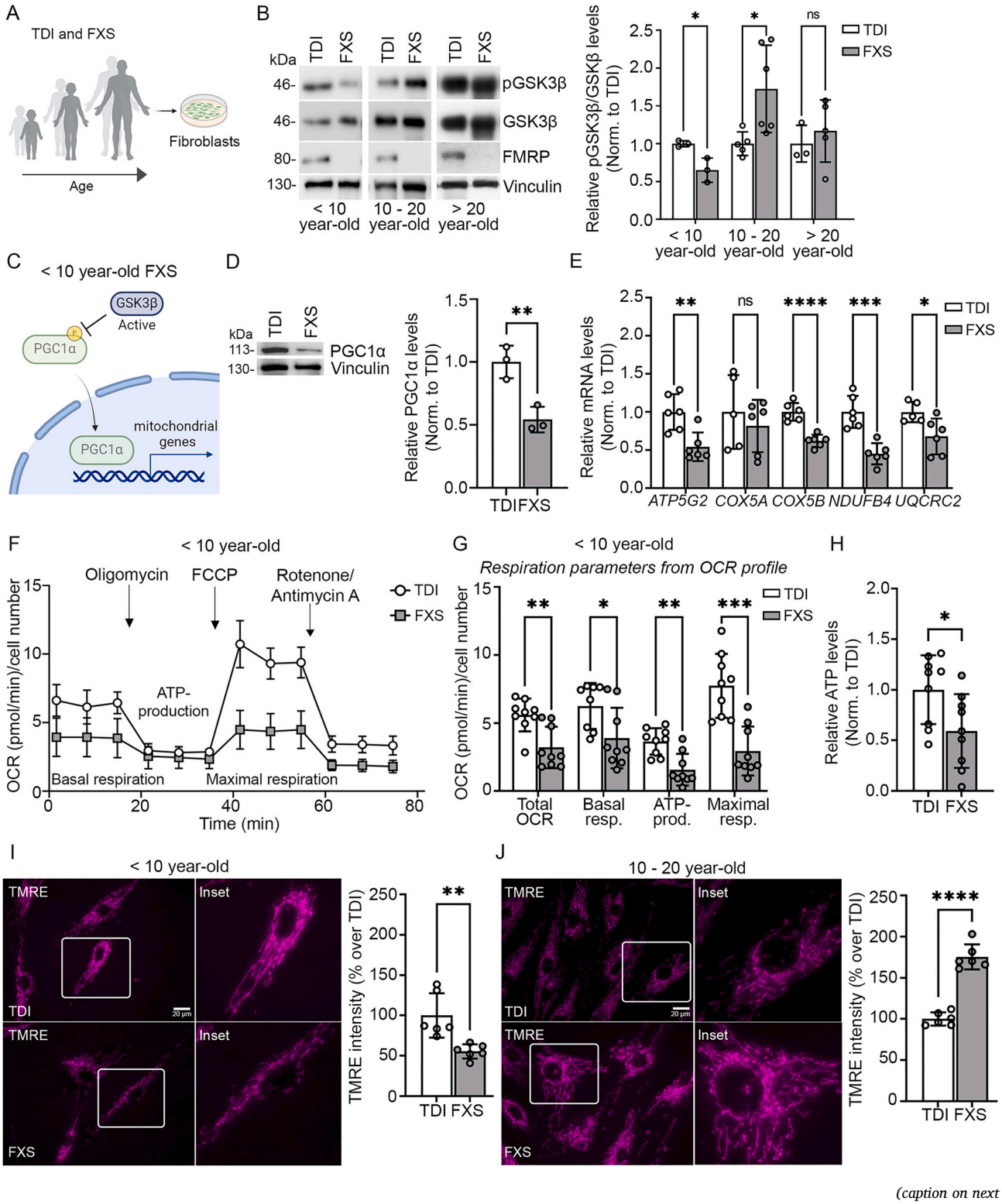

(caption on next page)

Fig. 3. GSK3β and mitochondrial activity in human cells from TDI and FXS. (A) Scheme of the experimental design. Human fibroblasts derived from TDI and FXS individuals with different age (image created in *BioRender.com*). (B) Left, representative Western blots showing pGSK3β (S9), GSK3β and FMRP levels in TDI and FXS fibroblasts stratified according to the age. Vinculin was used as loading control. Right, the bar plots show the quantification of pGSK3β (S9) normalized to GSK3β total levels. Each dot represents the average of a minimum of three technical replicates per individual. Error bars represent the SD (* $p < 0.05$, ns = non-significant, Multiple Student's *t*-test) (< 10-year-old TDI $n = 3$; FXS $n = 3$; 10–20 year-old TDI $n = 5$; FXS $n = 6$; > 20 year-old TDI $n = 3$; FXS $n = 5$). (C) Schematic representation of GSK3β - PGC1α pathway (image created in *BioRender.com*). (D) Representative Western blot showing PGC1α levels in young TDI and FXS fibroblasts. Vinculin was used as loading control. The bar plots show the quantification of PGC1α. Each dot represents the average of three technical replicates per individual. Error bars represent the SD (** $p < 0.01$, Student's *t*-test) (TDI $n = 3$; FXS $n = 3$). (E) The bar plots represent the quantification of *ATP5G2*, *COX5A*, *COX5B*, *NDFUB4* and *UQCRC2* mRNA levels in young FXS fibroblasts, normalized to *HPRT1* mRNA levels. Each dot represents a technical replicate. Error bars represent the SD (**** $p < 0.0001$, *** $p < 0.001$, ** $p < 0.01$, * $p < 0.05$, ns = non-significant, Multiple Student's *t*-test) (n = 5-65 technical replicates of 3 individuals per group; TDI $n = 3$; FXS $n = 3$). (F) Real-time Oxygen Consumption Rate (OCR) was measured in TDI and FXS fibroblasts using the Seahorse XFp Analyzer. Measurements were taken before (basal) and upon sequential injections of oligomycin, carbonyl cyanide p-(trifluoromethoxy) phenylhydrazone (FCCP), rotenone, and antimycin A. Each dot represents the average of a technical triplicate per individual. Error bars represent the SD (TDI $n = 3$; FXS $n = 3$). (G) The bar plots represent the total OCR and the rate of basal, ATP-linked, and maximal respiration calculated from OCR profile. Each dot represents a technical replicate. Error bars represent the SD (*** $p < 0.001$, ** $p < 0.01$, * $p < 0.05$, Multiple Student's *t*-test) (n = 8–9 technical replicates of 3 individuals; TDI $n = 3$; FXS $n = 3$). (H) The bar plots show the quantification of ATP levels in in young TDI and FXS fibroblasts. Error bars represent the SD (* $p < 0.05$, Student's *t*-test) ($n = 9$ technical replicates of 3 individuals per group; TDI $n = 3$; FXS $n = 3$). (I-J) Representative live images of TMRE fluorescence in young (I) and adolescent (J) TDI and FXS fibroblasts. The bar plots show the quantification of TMRE fluorescence intensity, indicating the mitochondrial membrane potential. Each dot represents a technical replicate. Error bars represent the SD (**** $p < 0.0001$, ** $p < 0.01$, Student's *t*-test) ($n = 6$ technical replicates of 3 individuals per group; TDI $n = 3$; FXS $n = 3$). Scale bar = 20 μm.

OCR (Fig. 3F-G), suggesting compromised mitochondrial function. Further analysis of the OCR profile revealed a decrease in basal respiration, ATP-linked respiration, and maximal respiration capacity (Fig. 3G), indicative of impaired energy production. Additionally, ELISA measurements corroborate the impaired mitochondrial function showing a significant reduction in ATP levels in FXS fibroblasts compared to age-matched TDI (Fig. 3H). To further investigate the mitochondrial defect, we used TMRE, a cell-permeable fluorescent dye that selectively labels active mitochondria in a membrane potential-dependent manner, due to its positive charge and the relative negative charge of mitochondria (Crowley et al., 2016). Consistent with the OCR data, young FXS fibroblasts displayed a remarkable reduction in mitochondrial membrane potential compared to TDI, indicating disruption of mitochondrial activity (Fig. 3I). Interestingly, fibroblasts from individuals with FXS in the 10–20 age group (group 2) exhibited increased TMRE intensity compared to TDI (Fig. 3J). This finding might be related to the previously observed decrease in GSK3β activity in this age group, suggesting a potential regulatory role of GSK3β in mitochondrial function during FXS progression.

3.4. Inhibition of GSK3β rescues mitochondrial activity in FXS fibroblasts

To evaluate a potential mitigation of the observed mitochondrial defects, FXS fibroblasts from young FXS individuals as well as from controls, were treated with the GSK3 inhibitor AFC05976, aiming at reducing GSK3β activity (Fig. 4A). At first, upon treatment, we validated the expression of β-catenin, a well-known GSK3β target that is phosphorylated by GSK3β with a consequent proteasomal degradation (Shah and Kazi, 2022) (Fig. S4C).

To define the optimal dose for the AFC05976 treatment, FXS fibroblasts were treated with different concentrations of the compound (see Materials and Methods) and the levels of β-catenin were measured after 24 h of treatment. Significant increase of β-catenin was observed after treatment with 0.3 μM of GSK3 inhibitor AFC05976 (Fig. S4D). Interestingly, reduced β-catenin levels were observed in fibroblasts derived from young FXS individuals, compared to TDI, and treatment with 0.3 μM AFC05976 restored β-catenin levels in FXS cells (Fig. S4E).

To determine if GSK3β inhibition corrects mitochondrial function, the levels of PGC1α, PGC1α-regulated mitochondrial genes, and organelle activity were assessed following the treatment. In fibroblasts from young FXS individuals, we observed a rescue of PGC1α levels (Fig. 4B) and a consequent substantial increase in *COX5B* and *NDUFB4* mRNA expression upon treatment with 0.3 μM of the GSK3 inhibitor AFC05976 (Fig. 4C), suggesting a potential restoration of complex I and IV activity. Interestingly, a similar increase in *COX5B* levels was also observed in TDI fibroblasts, suggesting a broad effect of the compound on PGC1α-dependent gene expression.

To investigate whether the restored expression of nuclear-encoded mitochondrial genes correlates with improved mitochondrial activity in FXS, the TMRE assay was performed post-treatment with the GSK3 inhibitor (Fig. 4D). The treatment restores mitochondrial function in FXS fibroblasts, as assessed by the significant increase in TMRE signal upon GSK3β inhibition (Fig. 4D). These results suggest that the modulation of GSK3β activity ameliorates mitochondrial alterations in fibroblasts from young FXS individuals, offering potential future avenues for targeted therapeutic interventions.

4. Discussion

In this study, we explore the expression and activity of GSK3β in FXS and its potential impact on mitochondrial function. An age-dependent dysregulation of GSK3β activity is revealed in both murine and human models of FXS, resulting in impaired expression of PGC1α, mitochondria-related genes and mitochondrial function, particularly at young age. Importantly, inhibition of GSK3β activity corrects the expression of GSK3β substrates, namely PGC1α and β-catenin as well as the observed mitochondrial defects in FXS human fibroblasts.

Developmental dysregulation of GSK3β activity at synapses of Fmr1 KO mice. Our study demonstrates a dynamic regulation of GSK3β activity at FXS synapses. As previously reported, in physiological condition, the murine brain exhibits dynamic fluctuations in GSK3β levels and phosphorylation throughout development (Beurel et al., 2012; Krishnankutty et al., 2017), highlighting its versatile role in regulating brain development and activity. While prior research documented hyperactive GSK3β in adult FXS mice (Franklin et al., 2014; Min et al., 2009), we reveal a critical early-stage dysregulation. Specifically, GSK3β is hyperactive in FXS cortical and hippocampal synapses at early postnatal stages, followed by a subsequent hypoactivity at later stages. This novel pattern of GSK3β dysregulation in FXS may be a key contributor to the synaptic deficits observed in FXS, including abnormal dendritic spine morphology and density (Bagni and Zukin, 2019; Gredell et al., 2023; Mercaldo et al., 2023).

A few studies have shown that inhibiting GSK3β restores synaptic morphology and function in the *Fmr1* KO mouse (Guo et al., 2011; Westmark et al., 2021), highlighting the potential of GSK3β in regulating spine phenotypes. Reduction or overexpression of GSK3β in the cortex and hippocampus affects spine density, stability, and maturation, as well as synaptic plasticity (Banach et al., 2022; Jaworski et al., 2019; Kondratiuk et al., 2017; Liu et al., 2017; Ochs et al., 2015; Wang et al., 2019). Increased GSK3β activity hampers spine maturation, leading to more immature spines (Banach et al., 2022; Kondratiuk et al., 2017). Likewise, decreased GSK3β activity disrupts spine formation, ultimately affecting synaptic plasticity (Bradley et al., 2012; Jaworski et al., 2019; Kondratiuk et al., 2017; Liu et al., 2017; Moreno-Jiménez et al., 2023;

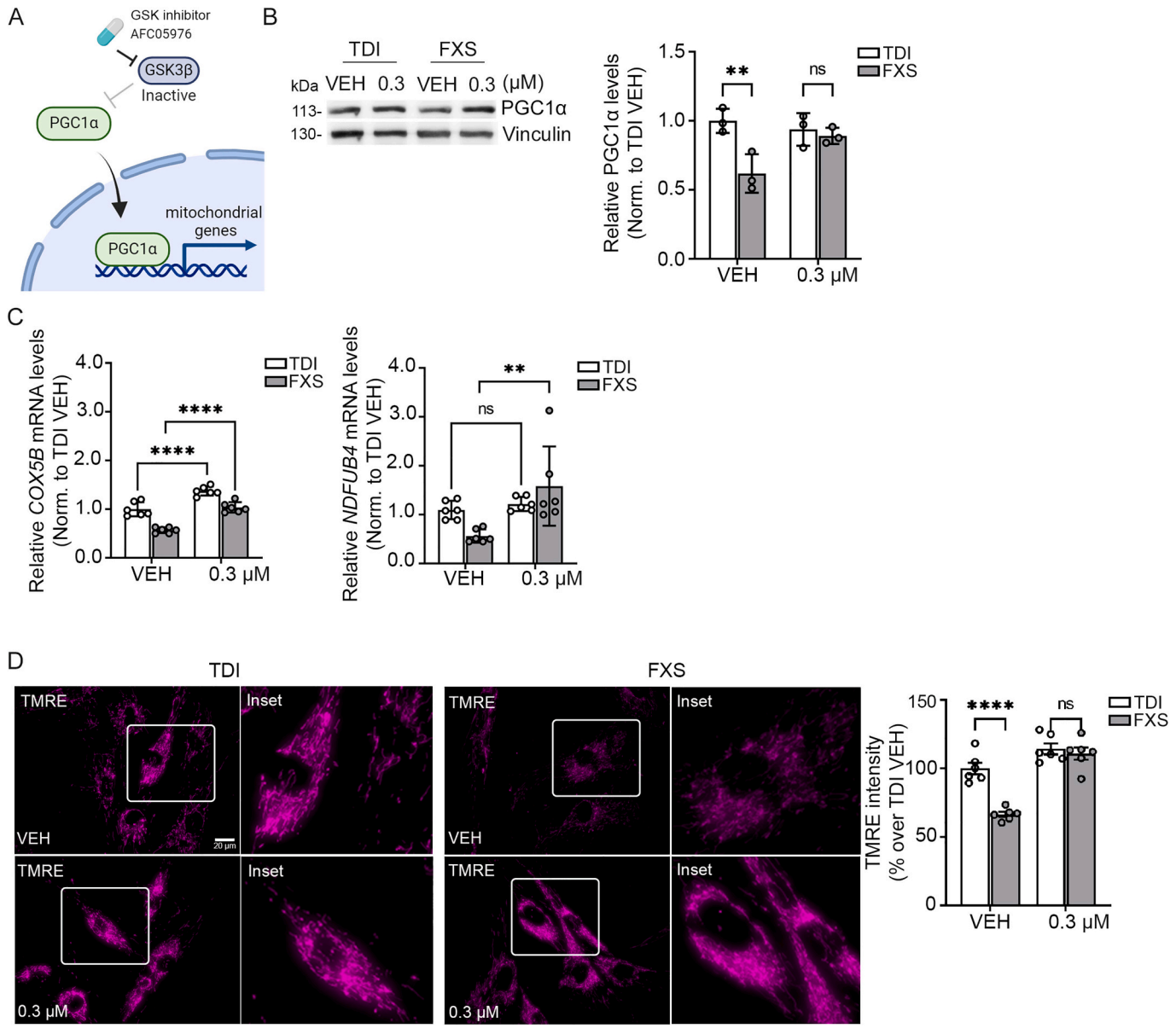

Fig. 4. Modulation of GSK3β activity in TDI and FXS human cells. (A) Schematic representation of the mechanism of action of the GSK3 inhibitor (image created in *BioRender.com*). (B) Left, representative Western blot showing PGC1α levels in young TDI and FXS human fibroblasts treated with DMSO (vehicle, VEH) or 0.3 μM GSK3 inhibitor AFC05976. Vinculin was used as loading control. Right, the bar plots show the quantification of PGC1α levels. Each dot represents the average of three technical replicates per individual. Error bars represent the SD (Two-way ANOVA analysis: treatment effect $F_{(1, 8)} = 2.974$, $p > 0.05$, genotype effect $F_{(1, 8)} = 12.33$, $p < 0.01$, interaction effect $F_{(1, 8)} = 7.541$, $p < 0.05$) (** $p < 0.01$, ns = non-significant, Sidak's multiple comparisons test) (TDI $n = 3$; FXS $n = 3$). (C) The bar plots represent the quantification of *COX5B* and *NDFUB4* mRNAs upon treatment with DMSO (vehicle, VEH) or 0.3 μM GSK3β inhibitor AFC05976 in young FXS fibroblasts, normalized to *HPRT1* mRNA levels. Each dot represents a technical replicate. Error bars represent the SD (Two-way ANOVA analysis *COX5B*: treatment effect $F_{(1, 20)} = 95.41$ $p < 0.0001$, genotype effect $F_{(1, 20)} = 79.51$, $p < 0.0001$, interaction effect $F_{(1, 20)} = 1.215$, $p > 0.05$) (**** $p < 0.0001$, ns = non-significant, Sidak's multiple comparisons test) (Two-way ANOVA analysis; *NDFUB4:* treatment effect $F_{(1, 20)} = 10.71$, $p < 0.01$, genotype effect $F_{(1, 20)} = 0.2223$, $p > 0.05$, interaction effect $F_{(1, 20)} = 6.591$, $p < 0.05$) (** $p < 0.01$, Sidak's multiple comparisons test) ($n = 6$ technical replicates of 3 individuals per group; TDI $n = 3$; FXS $n = 3$). (D) Representative live images of TMRE fluorescence in young TDI and FXS fibroblasts treated with DMSO (vehicle, VEH) or 0.3 μM GSK3 inhibitor AFC05976. The bar plots show the quantification of TMRE fluorescence intensity. Each dot represents a technical replicate. Error bars represent the SD (Two-way ANOVA analysis: treatment effect $F_{(1, 20)} = 59.99$, $p < 0.0001$, genotype effect $F_{(1, 20)} = 23.94$, $p < 0.0001$, interaction effect $F_{(1, 20)} = 15.77$, $p < 0.001$) (**** $p < 0.0001$, ns = non-significant, Sidak's multiple comparisons test) ($n = 6$ technical replicates of 3 individuals per group; TDI $n = 3$; FXS $n = 3$). Scale bar = 20 μm.

Ochs et al., 2015). Similar to our findings, a rat model of schizophrenia exhibits early postnatal hyperactivation of GSK3β at P7, influencing spine density, adult working memory, and synaptic plasticity (Xing et al., 2016). These findings suggest that early GSK3β hyperactivation observed in our study might contribute to the abnormal synaptogenesis seen in FXS. Furthermore, reduced GSK3β activity during late postnatal development and adulthood may disrupt other critical brain functions, including synaptic refinement, neuronal circuit formation, and experience-dependent plasticity. This highlights the possibility that GSK3β dysfunction throughout development likely contributes to the multifaceted phenotypes observed in FXS.

GSK3β-dependent mitochondrial defects in FXS. GSK3β is known for its regulatory role in metabolic pathways, including its impact on mitochondrial function (Wang et al., 2022). In particular, GSK3β inhibition stimulates the master mitochondrial regulator, namely PGC1α. Interestingly, defects in PGC1α, associated with changes in mitochondria-

related gene expression, have been previously documented in other neurological disorders, including ASD, Down syndrome, Huntington's disease, and Parkinson's disease (Bam et al., 2021; Feng et al., 2021; McMeekin et al., 2021; Valenti and Vacca, 2023; Zahedi et al., 2023), suggesting that alterations in this pathway may ultimately affect neuronal development and function. In addition, a recent study reported a downregulation of PGC1α expression in a fly model of FXS and a downregulation of mitochondrial activity affecting circadian rhythm (Weisz et al., 2024). Of note, we reveal decreased PGC1α levels in P7 *Fmr1* KO mice compared to WT, while increasing in adult P120 mice, consistent with the observed age-dependent dysregulation of GSK3β activity. Since GSK3α activity at synapses is comparable between WT and *Fmr1* KO animals, the observed mitochondrial dysfunctions appear to be linked to the selective perturbation of GSK3β rather than a general impairment of both GSK3 isoforms. Moreover, the expression of mitochondrial genes involved in maintaining appropriate mitochondrial functions (Guan et al., 2022; Vercellino and Sazanov, 2022) are reduced in young FXS mice, switching to increased levels later in development. These data are in line with the deregulation of the GSK3β-PGC1α axis observed in this study. Notably, these defects, including decreased PGC1α levels and impaired mitochondrial activity, are mirrored in human fibroblasts derived from young FXS individuals.

Mitochondria exhibit developmental plasticity, comprising changes in their structure and function (Bahat and Gross, 2019; Brandt et al., 2017; Daum et al., 2013; Duarte et al., 2023; Fame and Lehtinen, 2021; Granath-Panelo and Kajimura, 2024; Thomas et al., 2019). The time-dependent mitochondrial changes are crucial to ensure the adequate supply of energy throughout various stages of life. During early neuronal development, there is increased neuronal activity, accompanied by a transition of metabolism from glycolytic to oxidative phosphorylation (Fame and Lehtinen, 2021). In contrast, during aging, mitochondrial activity decreases due to reactive oxygen species (ROS) production (Gómez et al., 2023). However, in FXS, this finely tuned process may be disrupted. Our findings suggest that GSK3β hyperactivation at early stages lead to a reduction in mitochondria activity and ATP production. This energy deficit can hinder critical processes like neurotransmitter release, reuptake, and proper signal transmission, ultimately resulting in synaptic defects. In the later stages of mouse brain development, we observe enhanced expression of three of the six analyzed mRNAs (*Atp5g2, Cox5b* and *Ndufb4*). Based on our findings on PGC1α expression, the observed difference of the nuclear-encoded mitochondrial gene expression may be associated with fluctuation in PGC1α expression, consistent with prior evidence (Martin et al., 2016).

In addition to its role in the regulation of PGC1α, active GSK3β contributes to mitochondrial dysfunction by leading to rapid and unregulated opening of the mitochondrial permeability transition pore (mPTP) and consequent dissipation of proton gradient and inefficient ATP production (Zhu et al., 2013). This mechanism likely exacerbates the mitochondrial defects observed in young FXS individuals.

Overall, the intricate interplay between GSK3β and PGC1α highlights the fine regulatory mechanisms that affect the functional and structural changes of mitochondria. Among the numerous signaling pathways involved, fluctuations in GSK3β activity may play a significant role, and any perturbation of its finely tuned activity may underscore pathological mitochondrial defects.

Use of GSK3β inhibitor for FXS treatment. Previous evidence indicates that GSK3α hyperactivation in total extracts is more prevalent across different brain regions in adult *Fmr1* KO animals compared to GSK3β dysregulation (Min et al., 2009; Yuskaitis et al., 2010). Few studies have demonstrated that GSK3 (α/β) inhibitors, such as lithium, can effectively improve adult FXS phenotypes (Rizk et al., 2021). However, while a selective GSK3β inhibitor was ineffective in adults, specific inhibition of GSK3α significantly improved FXS-related phenotypes (McCamphill et al., 2020). Our findings show that GSK3β hyperactivation is an early developmental event that transitions to hypoactivity in adulthood. Based on previous findings, we propose a dual mode of action for GSK3 inhibitors: GSK3β inhibition is effective at a young age, while GSK3α inhibition is beneficial in adulthood.

Despite the limited exploration of GSK3 inhibition as a treatment for FXS in clinical trials, an open-label study with lithium (Berry-Kravis et al., 2008) offered promising results. This study found that participants showed significant improvement in several domains of behavior as measured by standardized assessments including better management of difficult behaviors, and enhanced learning abilities (Berry-Kravis et al., 2008). Encouragingly, GSK3β inhibition with lithium has shown positive results in bipolar disorder and schizophrenia (Fountoulakis et al., 2022; Janiri et al., 2023), and clinical trials are ongoing for Alzheimer's disease (Devanand et al., 2022). This suggests that GSK3β inhibition may be a viable strategy for treating neurological conditions including FXS. However, lithium has limitations. Its broad mechanism of action can lead to side effects, making it a less desirable therapeutic option for children and adolescents with FXS and other neurodevelopmental disorders (Arciniegas Ruiz and Eldar-Finkelman, 2021; Ferensztajn-Rochowiak and Rybakowski, 2023; Mintz and Hollenberg, 2019; Siegel et al., 2014). The GSK3 inhibitor AFC05976 used in our study shows potential for therapeutic strategies targeting excessive GSK3β activity during a critical developmental window. The inhibition of GSK3β activity at an early age restores the levels of its substrates, β-catenin and PGC1α, as well as mitochondrial defects. Moreover, AFC05976 can cross the blood-brain barrier (Buonfiglio et al., 2020), facilitating targeted CNS therapy.

Despite the efforts in recent years, no treatments are currently approved for FXS (Protic and Hagerman, 2024). The context of FXS is further complicated by the diversity in genetic profiles, clinical manifestations, and temporal variation, resulting in individuals exhibiting a wide range of clinical and molecular features (Cencelli et al., 2023; Cregenzán-Royo et al., 2022; Elhawary et al., 2023; Verdura et al., 2021). Identifying a specific temporal window and subgroups of FXS individuals who may benefit from targeted therapy is crucial to minimize side effects and optimize treatment timing. We observe age-dependent deregulation of GSK3β and mitochondrial activity in human FXS fibroblasts: hyperactivation of GSK3β and decreased mitochondrial activity (reduced OCR and mitochondrial membrane potential) in young individuals, followed by downregulation during adolescence, consistent with the findings in the murine model. Although the number of cell lines used in this study is limited, the absence of dysregulated GSK3β activity in iPSC-derived neurons supports the idea that GSK3β dysregulation occurs primarily during postnatal development. Of note, human iPSC-derived neurons are typically considered to correspond to a prenatal stage of maturation and may not fully represent the complexities of postnatal neuronal development (Espuny-Camacho et al., 2013). This developmental immaturity could account for the absence of significant differences in pGSK3β levels. We cannot exclude that xenograft transplantation into murine brains, promoting neuronal maturation and connectivity (Linaro et al., 2019), a proxy for an *in vivo* enviroment, would lead to a more mature phenotype of iPSC-derived neurons exhibiting a similar GSK3β dysregulation as observed in murine synaptoneurosomes.

The use of fibroblasts in this context represents a valuable tool for studying the effects of age on gene expression because they maintain the epigenetic signature reflecting the donor's age (Fleischer et al., 2018; Ivanov et al., 2016; Rorteau et al., 2022). Furthermore, our previous work has shown that fibroblasts effectively recapitulate the molecular defects observed in neurons, making them a powerful tool for investigating FXS pathology (Jacquemont et al., 2018). Despite the limited sample size, our findings indicate that GSK3 inhibition restores both mitochondrial gene expression and function in fibroblasts derived from young FXS individuals.

5. Limitations of the study

We acknowledge some limitations of this study. First, in the murine model, we observe dysregulation of the GSK3β-PGC1α axis at synapses using synaptoneurosome preparations. While this experiment provide evidence for a synaptic dysregulation, we cannot exclude possible alterations in other cellular compartments such as the soma or along axons and dendrites. Moreover, data on purified synaptoneurosomes do not provide information on cell identity, *i.e.* whether the observed dysregulation of the GSK3β-PGC1α axis belongs to either glutamatergic or GABAergic neurons. Second, our data suggest that dysregulated GSK3β activity contributes to a mitochondrial dysfunction in FXS. The metabolic effects of GSK3β inhibition have been linked to enhanced stabilization of the PGC1α protein and improved mitochondrial metabolism (Martin et al., 2018). To the best of our knowledge, there is no direct evidence linking GSK3α to PGC1α regulation or mitochondrial function. However, as GSK3α and GSK3β share structural and functional similarities, we cannot entirely rule out a potential contribution of GSK3α to PGC1α stability and/or mitochondrial activity. Therefore, additional experiments are required to address the specific role of GSK3β in the FXS-associated mitochondrial dysfunction.

6. Conclusions

Despite some limitations, our study provides the evidence in rodent and human cells supporting the involvement of GSK3β in mitochondrial dysfunction in FXS, in a developmental specific manner. Furthermore, the inhibition of GSK3 restored mitochondrial gene expression and activity, suggesting a potential strategy for targeted therapeutic interventions during a specific developmental window in FXS. While these results offer a promising avenue for personalized treatment strategies, further research is required to elucidate the interplay between GSK3β dysregulation, mitochondrial dysfunction, and FXS pathogenesis.

Fundings

This work was supported by Telethon GGP20137, Angelini Pharma S.p.A., Next Generation EU – PRIN 20227JA8R3, NEXTGENERATIONEU (NGEU) National Recovery and Resilience Plan (NRRP), project MNESYS (PE0000006) – A Multiscale integrated approach to the study of the nervous system in health and disease (DN. 1553 11.10.2022), Unione europea – FSE REACT-EU, PON Ricerca e Innovazione 2014-2020 and SNSF 310030 - 215706.

Authors' contributions

GC and CB conceived the study. GC, GP, CR, ER, GCe, AG and GA performed the experiments and/or analyzed the data. CB and LP supervised the study. BG, RO, IC, FP, and CM provide the drug. GC and CB wrote the manuscript with input from all authors. All authors have read and agreed to the published version of the manuscript.

Declaration of Generative AI and AI assisted technologies in the writing process

During the preparation of this work the authors used ChatGPT 3.5 or ChatGPT4.o to improve language and readability. After using this tool, the authors reviewed and edited the content as needed and takes full responsibility for the content of the publication.

CRediT authorship contribution statement

Giulia Cencelli: Conceptualization, Investigation, Formal analysis, Visualization, Writing – original draft, Review & editing. **Giorgia Pedini**: Investigation, Formal analysis, Visualization, Review & editing. **Carlotta Ricci**: Investigation, Formal analysis. Eleonora Rosina: Investigation, Formal analysis, Review & editing. **Giorgia Cecchetti**: Investigation, Formal analysis. **Antonietta Gentile**: Formal analysis, Review & editing. **Giuseppe Aiello**: Formal analysis, Review & editing. **Laura Pacini**: Supervision. **Beatrice Garrone**: Resources. **Rosella Ombrato**: Resources. **Isabella Coletta**: Resources. **Federica Prati**: Resources. **Claudio Milanese**: Resources. **Claudia Bagni**: Conceptualization, Supervision, Project administration, Funding acquisition, Writing – original draft, Review & editing.

Declaration of competing interest

The authors declare the following financial interests/personal relationships which may be considered as potential competing interests:

Claudia Bagni reports financial support by Angelini SpA. Beatrice Garrone, Rosella Ombrato, Isabella Coletta, Federica Prati, Claudio Milanese are employees at Angelini Pharma S.p.A.The other authors have no known competing financial interests or personal relationships that could have appeared to influence the work reported in this paper.

Data availability

The datasets used and/or analyzed during the current study available from the corresponding author on reasonable request.

Acknowledgements

The authors are grateful to Sebastien Jacquemont, Rob Willemsen and Flora Tassone for generously providing the FXS fibroblast cell lines described in (Jacquemont et al., 2018). We thank Randi Hagerman for patients' recruitment and Philip H. Schwartz for cell culture and iPSC-derivation. Additionally, the authors thank Valentina Mercaldo and Adrian C. Lo for providing preliminary data, Tilmann Achsel and Massimo Regoli for statistical consulting, Alexandros Kanellopoulos for scientific discussions, and Maria Giulia Farace for the critical reading of the manuscript. The graphical abstract and the drawings of the Figures were created with BioRender.com.

Appendix A. Supplementary data

Supplementary data to this article can be found online at https://doi.org/10.1016/j.nbd.2024.106726.

References

Acero-Garcés, D.O., Saldarriaga, W., Cabal-Herrera, A.M., Rojas, C.A., Hagerman, R.J., 2023. Fragile X syndrome in children. Colomb. Medica Cali, Colomb. 54, e4005089.
Anderson, R.M., Barger, J.L., Edwards, M.G., Braun, K.H., O'Connor, C.E., Prolla, T.A., Weindruch, R., 2008. Dynamic regulation of PGC-1alpha localization and turnover implicates mitochondrial adaptation in calorie restriction and the stress response. Aging Cell 7, 101–111.
Anitha, A., Nakamura, K., Thanseem, I., Matsuzaki, H., Miyachi, T., Tsujii, M., Iwata, Y., Suzuki, K., Sugiyama, T., Mori, N., 2013. Downregulation of the expression of mitochondrial electron transport complex genes in autism brains. Brain Pathol. 23, 294–302.
Anitha, A., Thanseem, I., Iype, M., Thomas, S.V., 2023. Mitochondrial dysfunction in cognitive neurodevelopmental disorders: cause or effect? Mitochondrion 69, 18–32.
Arciniegas Ruiz, S.M., Eldar-Finkelman, H., 2021. Glycogen synthase Kinase-3 inhibitors: preclinical and clinical focus on CNS-A decade onward. Front. Mol. Neurosci. 14, 792364.
Bagni, C., Zukin, R.S., 2019. A synaptic perspective of Fragile X syndrome and autism Spectrum disorders. Neuron 101, 1070–1088.
Bahat, A., Gross, A., 2019. Mitochondrial plasticity in cell fate regulation. J. Biol. Chem. 294, 13852–13863.
Bakker, C.E., Verheij, C., Willemsen, R., van der Helm, R., Oerlemans, F., Vermey, M., Bygrave, A., Hoogeveen, A.T., Oostra, B.A., et al., 1994. Fmr1 knockout mice: a model to study fragile X mental retardation. Cell 78, 23–33.
Bam, S., Buchanan, E., Mahony, C., O'Ryan, C., 2021. DNA methylation of PGC-1α is associated with elevated mtDNA copy number and altered urinary metabolites in autism Spectrum disorder. Front. Cell Dev. Biol. 9, 696428.
Banach, E., Jaworski, T., Urban-Ciećko, J., 2022. Early synaptic deficits in GSK-3β overexpressing mice. Neurosci. Lett. 784, 136744.

Belenguer, P., Duarte, J.M.N., Schuck, P.F., Ferreira, G.C., 2019. Mitochondria and the brain: bioenergetics and beyond. Neurotox. Res. 36, 219–238.
Berry-Kravis, E., Sumis, A., Hervey, C., Nelson, M., Porges, S.W., Weng, N., Weiler, I.J., Greenough, W.T., 2008. Open-label treatment trial of lithium to target the underlying defect in fragile X syndrome. J. Dev. Behav. Pediatr. 29, 293–302.
Beurel, E., Mines, M.A., Song, L., Jope, R.S., 2012. Glycogen synthase kinase-3 levels and phosphorylation undergo large fluctuations in mouse brain during development. Bipolar Disord. 14, 822–830.
Beurel, E., Grieco, S.F., Jope, R.S., 2015. Glycogen synthase kinase-3 (GSK3): regulation, actions, and diseases. Pharmacol. Ther. 148, 114–131.
Bradley, C., Peineau, S., Taghibiglou, C., Nicolas, C., Whitcomb, D., Bortolotto, Z., Kaang, B.-K., Cho, K., Wang, Y.-T., Collingridge, G., 2012. A Pivotal Role of GSK-3 in Synaptic Plasticity. Front. Mol, Neurosci, p. 5.
Brandt, T., Mourier, A., Tain, L.S., Partridge, L., Larsson, N.-G., and Kühlbrandt, W. (2017). Changes of mitochondrial ultrastructure and function during ageing in mice and \textit{Drosophila}. Elife 6, e24662.
Brick, D.J., Nethercott, H.E., Montesano, S., Banuelos, M.G., Stover, A.E., Schutte, S.S., O'Dowd, D.K., Hagerman, R.J., Ono, M., Hessl, D.R., et al., 2014. The autism Spectrum disorders stem cell resource at Children's Hospital of Orange County: implications for disease modeling and drug discovery. Stem Cells Transl. Med. 3, 1275–1286.
Bülow, P., Zlatic, S.A., Wenner, P.A., Bassell, G.J., Faundez, V., 2021a. FMRP attenuates activity dependent modifications in the mitochondrial proteome. Mol. Brain 14, 75.
Bülow, P., Wenner, P.A., Faundez, V., Bassell, G.J., 2021b. Mitochondrial structure and polarity in dendrites and the axon initial segment are regulated by homeostatic plasticity and dysregulated in Fragile X syndrome. Front. Cell Dev. Biol. 9, 702020.
Buonfiglio, R., Prati, F., Bischetti, M., Cavarischia, C., Furlotti, G., Ombrato, R., 2020. Discovery of novel Imidazopyridine GSK-3β inhibitors supported by computational approaches. Molecules 25.
Cabral-Costa, J.V., Kowaltowski, A.J., 2020. Neurological disorders and mitochondria. Mol. Asp. Med. 71, 100826.
Cencelli, G., Pacini, L., De Luca, A., Messia, I., Gentile, A., Kang, Y., Nobile, V., Tabolacci, E., Jin, P., Farace, M.G., et al., 2023. Age-dependent dysregulation of APP in neuronal and skin cells from Fragile X individuals. Cells 12, 758.
Chen, L., Qin, Y., Liu, B., Gao, M., Li, A., Li, X., Gong, G., 2022. PGC-1α-mediated mitochondrial quality control: molecular mechanisms and implications for heart failure. Front. Cell Dev. Biol. 10, 871357.
Ch'ng, C., Kwok, W., Rogic, S., and Pavlidis, P., 2015. Meta-analysis of gene expression in autism Spectrum disorder. Autism res. Off. J. Int. Soc. Autism Res. 8, 593–608.
Cisneros-Franco, J.M., Voss, P., Thomas, M.E., de Villers-Sidani, E., 2020. Chapter 8 - critical periods of brain development. In: Gallagher, A., Bulteau, C., Cohen, D., J.L.B. T.-H. of C.N. Michaud (Eds.), Neurocognitive Development: Normative Development. Elsevier, pp. 75–88.
Clemente-Suárez, V.J., Redondo-Flórez, L., Beltrán-Velasco, A.I., Ramos-Campo, D.J., Belinchón-deMiguel, P., Martinez-Guardado, I., Dalamitros, A.A., Yáñez-Sepúlveda, R., Martín-Rodríguez, A., Tornero-Aguilera, J.F., 2023. Mitochondria and brain disease: a comprehensive review of pathological mechanisms and therapeutic opportunities. Biomedicines 11, 1–52.
Cregenzán-Royo, O., Brun-Gasca, C., Fornieles-Deu, A., 2022. Behavior problems and social competence in Fragile X syndrome: a systematic review. Genes (Basel) 13, 280.
Crowley, L.C., Christensen, M.E., Waterhouse, N.J., 2016. Measuring mitochondrial transmembrane potential by TMRE staining. Cold Spring Harb Protoc 2016.
D'Antoni, S., de Bari, L., Valenti, D., Borro, M., Bonaccorso, C.M., Simmaco, M., Vacca, R. A., Catania, M.V., 2020. Aberrant mitochondrial bioenergetics in the cerebral cortex of the Fmr1 knockout mouse model of fragile X syndrome. Biol. Chem. 401, 497–503.
Daum, B., Walter, A., Horst, A., Osiewacz, H.D., Kühlbrandt, W., 2013. Age-dependent dissociation of ATP synthase dimers and loss of inner-membrane cristae in mitochondria. Proc. Natl. Acad. Sci. USA 110, 15301–15306.
Dehorter, N., Del Pino, I., 2020. Shifting developmental trajectories during critical periods of brain formation. Front. Cell. Neurosci. 14.
Devanand, D.P., Crocco, E., Forester, B.P., Husain, M.M., Lee, S., Vahia, I.V., Andrews, H., Simon-Pearson, L., Imran, N., Luca, L., et al., 2022. Low dose Lithium treatment of behavioral complications in Alzheimer's disease: lit-AD randomized clinical trial. Am. J. Geriatr. Psychiatry off. J. Am. Assoc. Geriatr. Psychiatry 30, 32–42.
D'Incal, C., Broos, J., Torfs, T., Kooy, R.F., Vanden Berghe, W., 2022. Towards kinase inhibitor therapies for Fragile X syndrome: tweaking twists in the autism Spectrum kinase signaling network. Cells 11, 1325.
Duarte, F.V., Ciampi, D., Duarte, C.B., 2023. Mitochondria as central hubs in synaptic modulation. Cell. Mol. Life Sci. 80, 173.
Elhawary, N.A., AlJahdali, I.A., Abumansour, I.S., Azher, Z.A., Falemban, A.H., Madani, W.M., Alosaimi, W., Alghamdi, G., Sindi, I.A., 2023. Phenotypic variability to medication management: an update on fragile X syndrome. Hum. Genomics 17, 60.
Espuny-Camacho, I., Michelsen, K.A., Gall, D., Linaro, D., Hasche, A., Bonnefont, J., Bali, C., Orduz, D., Bilheu, A., Herpoel, A., et al., 2013. Pyramidal neurons derived from human pluripotent stem cells integrate efficiently into mouse brain circuits in vivo. Neuron 77, 440–456.
Fame, R.M., Lehtinen, M.K., 2021. Mitochondria in early forebrain development: from neurulation to mid-Corticogenesis. Front. Cell Dev. Biol. 9, 780207.
Faria-Pereira, A., Morais, V.A., 2022. Synapses: the Brain's energy-demanding sites. Int. J. Mol. Sci. 23, 3627.
Feng, C., Chen, Y., Zhang, Y., Yan, Y., Yang, M., Gui, H., Wang, M., 2021. PTEN regulates mitochondrial biogenesis via the AKT/GSK-3β/PGC-1α pathway in autism. Neuroscience 465, 85–94.
Ferensztajn-Rochowiak, E., Rybakowski, J.K., 2023. Long-term Lithium therapy: side effects and interactions. Pharmaceuticals (Basel) 16, 74.
Fleischer, J.G., Schulte, R., Tsai, H.H., Tyagi, S., Ibarra, A., Shokhirev, M.N., Huang, L., Hetzer, M.W., Navlakha, S., 2018. Predicting age from the transcriptome of human dermal fibroblasts. Genome Biol. 19, 221.
Föcking, M., Dicker, P., Lopez, L.M., Hryniewiecka, M., Wynne, K., English, J.A., Cagney, G., Cotter, D.R., 2016. Proteomic analysis of the postsynaptic density implicates synaptic function and energy pathways in bipolar disorder. Transl. Psychiatry 6, e959.
Fountoulakis, K.N., Tohen, M., Zarate, C.A.J., 2022. Lithium treatment of bipolar disorder in adults: a systematic review of randomized trials and meta-analyses. Eur. Neuropsychopharmacol. J. Eur. Coll. Neuropsychopharmacol. 54, 100–115.
Franklin, A.V., King, M.K., Palomo, V., Martinez, A., McMahon, L.L., Jope, R.S., 2014. Glycogen synthase kinase-3 inhibitors reverse deficits in long-term potentiation and cognition in fragile X mice. Biol. Psychiatry 75, 198–206.
Geng, J., Khaket, T.P., Pan, J., Li, W., Zhang, Y., Ping, Y., Cobos Sillero, M.I., Lu, B., 2023. Deregulation of ER-mitochondria contact formation and mitochondrial calcium homeostasis mediated by VDAC in fragile X syndrome. Dev. Cell 58, 597–615.e10.
Gómez, J., Mota-Martorell, N., Jové, M., Pamplona, R., Barja, G., 2023. Mitochondrial ROS production, oxidative stress and aging within and between species: evidences and recent advances on this aging effector. Exp. Gerontol. 174, 112134.
Gonzalez-Lozano, M.A., Klemmer, P., Gebuis, T., Hassan, C., van Nierop, P., van Kesteren, R.E., Smit, A.B., Li, K.W., 2016. Dynamics of the mouse brain cortical synaptic proteome during postnatal brain development. Sci. Rep. 6, 35456.
Granath-Panelo, M., and Kajimura, S. (2024). Mitochondrial heterogeneity and adaptations to cellular needs. Nat. Cell Biol. 26, 674–686.
Grandi, M., Galber, C., Gatto, C., Nobile, V., Pucci, C., Schaldemose Nielsen, I., Boldrin, F., Neri, G., Chiurazzi, P., Solaini, G., et al., 2024. Mitochondrial dysfunction causes cell death in patients affected by Fragile-X-associated disorders. Int. J. Mol. Sci. 25.
Gredell, M., Lu, J., Zuo, Y., 2023. The effect of single-cell knockout of Fragile X Messenger Ribonucleoprotein on synaptic structural plasticity. Front. Synaptic Neurosci 15.
Griffiths, K.K., Wang, A., Wang, L., Tracey, M., Kleiner, G., Quinzii, C.M., Sun, L., Yang, G., Perez-Zoghbi, J.F., Licznerski, P., et al., 2020. Inefficient thermogenic mitochondrial respiration due to futile proton leak in a mouse model of fragile X syndrome. FASEB. J. Off. Publ. Fed. Am. Soc. Exp. Biol. 34, 7404–7426.
Guan, S., Zhao, L., Peng, R., 2022. Mitochondrial respiratory chain Supercomplexes: from structure to function. Int. J. Mol. Sci. 23, 13880.
Guo, W., Murthy, A.C., Zhang, L., Johnson, E.B., Schaller, E.G., Allan, A.M., Zhao, X., 2011. Inhibition of GSK3β improves hippocampus-dependent learning and rescues neurogenesis in a mouse model of fragile X syndrome. Hum. Mol. Genet. 21, 681–691.
Hagerman, R.J., Berry-Kravis, E., Hazlett, H.C., Bailey, D.B., Moine, H., Kooy, R.F., Tassone, F., Gantois, I., Sonenberg, N., Mandel, J.L., et al., 2017. Fragile X syndrome. Nat. Rev. Dis. Prim. 3, 17065.
Hollis, F., Kanellopoulos, A.K., Bagni, C., 2017. Mitochondrial dysfunction in autism Spectrum disorder: clinical features and perspectives. Curr. Opin. Neurobiol. 45, 178–187.
Ivanov, N.A., Tao, R., Chenoweth, J.G., Brandtjen, A., Mighdoll, M.I., Genova, J.D., McKay, R.D., Jia, Y., Weinberger, D.R., Kleinman, J.E., et al., 2016. Strong components of epigenetic memory in cultured human fibroblasts related to site of origin and donor age. PLoS Genet. 12, e1005819.
Jacquemont, S., Pacini, L., Jønch, A.E., Cencelli, G., Rozenberg, I., He, Y., D'Andrea, L., Pedini, G., Eldeeb, M., Willemsen, R., et al., 2018. Protein synthesis levels are increased in a subset of individuals with fragile X syndrome. Hum. Mol. Genet. 27, 2039–2051.
Janiri, D., Sampogna, G., Albert, U., Caraci, F., Martinotti, G., Serafini, G., Tortorella, A., Zuddas, A., Fiorillo, A., Sani, G., 2023. Lithium use in childhood and adolescence, peripartum, and old age: an umbrella review. Int. J. Bipolar Disord. 11, 8.
Jaworski, T., Banach-Kasper, E., Gralec, K., 2019. GSK-3β at the intersection of neuronal plasticity and neurodegeneration. Neural Plast. 2019, 4209475.
Kanellopoulos, A.K., Mariano, V., Spinazzi, M., Woo, Y.J., McLean, C., Pech, U., Li, K.W., Armstrong, J.D., Giangrande, A., Callaerts, P., et al., 2020. Aralar sequesters GABA into hyperactive mitochondria, causing social behavior deficits. Cell 180, 1178–1197.e20.
Kondratiuk, I., Łęski, S., Urbańska, M., Biecek, P., Devijver, H., Lechat, B., Van Leuven, F., Kaczmarek, L., Jaworski, T., 2017. GSK-3β and MMP-9 cooperate in the control of dendritic spine morphology. Mol. Neurobiol. 54, 200–211.
Krishnankutty, A., Kimura, T., Saito, T., Aoyagi, K., Asada, A., Takahashi, S.-I., Ando, K., Ohara-Imaizumi, M., Ishiguro, K., Hisanaga, S., 2017. In vivo regulation of glycogen synthase kinase 3β activity in neurons and brains. Sci. Rep. 7, 8602.
Licznerski, P., Park, H.-A., Rolyan, H., Chen, R., Mnatsakanyan, N., Miranda, P., Graham, M., Wu, J., Cruz-Reyes, N., Mehta, N., et al., 2020. ATP synthase c-subunit leak causes aberrant cellular metabolism in Fragile X syndrome. Cell 182, 1170–1185.e9.
Linaro, D., Vermaercke, B., Iwata, R., Ramaswamy, A., Libé-Philippot, B., Boubakar, L., Davis, B.A., Wierda, K., Davie, K., Poovathingal, S., et al., 2019. Xenotransplanted human cortical neurons reveal species-specific development and functional integration into mouse visual circuits. Neuron 104, 972–986.e6.

Liu, E., Xie, A.-J., Zhou, Q., Li, M., Zhang, S., Li, S., Wang, W., Wang, X., Wang, Q., Wang, J.-Z., 2017. GSK-3β deletion in dentate gyrus excitatory neuron impairs synaptic plasticity and memory. Sci. Rep. 7, 5781.
Marosi, M., Arman, P., Aceto, G., D'Ascenzo, M., Laezza, F., 2022. Glycogen synthase kinase 3: ion channels, plasticity, and diseases. Int. J. Mol. Sci. 23, 4413.
Martin, S.A., DeMuth, T.M., Miller, K.N., Pugh, T.D., Polewski, M.A., Colman, R.J., Eliceiri, K.W., Beasley, T.M., Johnson, S.C., Anderson, R.M., 2016. Regional metabolic heterogeneity of the hippocampus is nonuniformly impacted by age and caloric restriction. Aging Cell 15, 100–110.
Martin, S.A., Souder, D.C., Miller, K.N., Clark, J.P., Sagar, A.K., Eliceiri, K.W., Puglielli, L., Beasley, T.M., Anderson, R.M., 2018. GSK3β regulates brain energy metabolism. Cell Rep. 23, 1922–1931.e4.
McCamphill, P.K., Stoppel, L.J., Senter, R.K., Lewis, M.C., Heynen, A.J., Stoppel, D.C., Sridhar, V., Collins, K.A., Shi, X., Pan, J.Q., et al., 2020. Selective Inhibition of Glycogen Synthase Kinase 3α Corrects Pathophysiology in a Mouse Model of Fragile X Syndrome. Sci. Transl, Med, p. 12.
McMeekin, L.J., Fox, S.N., Boas, S.M., Cowell, R.M., 2021. Dysregulation of PGC-1α-dependent transcriptional programs in neurological and developmental disorders: therapeutic challenges and opportunities. Cells 10, 352.
Mercaldo, V., Vidimova, B., Gastaldo, D., Fernández, E., Lo, A.C., Cencelli, G., Pedini, G., De Rubeis, S., Longo, F., Klann, E., et al., 2023. Altered striatal actin dynamics drives behavioral inflexibility in a mouse model of fragile X syndrome. Neuron 111, 1760–1775.e8.
Min, W.W., Yuskaitis, C.J., Yan, Q., Sikorski, C., Chen, S., Jope, R.S., Bauchwitz, R.P., 2009. Elevated glycogen synthase kinase-3 activity in Fragile X mice: key metabolic regulator with evidence for treatment potential. Neuropharmacology 56, 463–472.
Mintz, M., Hollenberg, E., 2019. Revisiting Lithium: utility for behavioral stabilization in adolescents and adults with autism Spectrum disorder. Psychopharmacol. Bull. 49, 28–40.
Mithal, D.S., Chandel, N.S., 2020. Mitochondrial dysfunction in Fragile-X syndrome: plugging the leak may save the ship. Mol. Cell 80, 381–383.
Moreno-Jiménez, E.P., Flor-García, M., Hernández-Vivanco, A., Terreros-Roncal, J., Rodríguez-Moreno, C.B., Toni, N., Méndez, P., Llorens-Martín, M., 2023. GSK-3β orchestrates the inhibitory innervation of adult-born dentate granule cells in vivo. Cell. Mol. Life Sci. 80, 225.
Nobile, V., Palumbo, F., Lanni, S., Ghisio, V., Vitali, A., Castagnola, M., Marzano, V., Maulucci, G., De Angelis, C., De Spirito, M., et al., 2020. Altered mitochondrial function in cells carrying a premutation or unmethylated full mutation of the FMR1 gene. Hum. Genet. 139, 227–245.
Ochs, S.M., Dorostkar, M.M., Aramuni, G., Schön, C., Filser, S., Pöschl, J., Kremer, A., Van Leuven, F., Ovsepian, S.V., Herms, J., 2015. Loss of neuronal GSK3β reduces dendritic spine stability and attenuates excitatory synaptic transmission via β-catenin. Mol. Psychiatry 20, 482–489.
Ozgen, S., Krigman, J., Zhang, R., Sun, N., 2022. Significance of mitochondrial activity in neurogenesis and neurodegenerative diseases. Neural Regen. Res. 17, 741–747.
Pekkurnaz, G., Wang, X., 2022. Mitochondrial heterogeneity and homeostasis through the lens of a neuron. Nat. Metab. 4, 802–812.
Prati, F., Buonfiglio, R., Furlotti, G., Cavarischia, C., Mangano, G., Picollo, R., Oggianu, L., di Matteo, A., Olivieri, S., Bovi, G., et al., 2020. Optimization of Indazole-based GSK-3 inhibitors with mitigated hERG issue and in vivo activity in a mood disorder model. ACS Med. Chem. Lett. 11, 825–831.
Protic, D., Hagerman, R., 2024. State-of-the-Art Therapies for Fragile X Syndrome. Dev. Med, Child Neurol.
Richter, J.D., Zhao, X., 2021. The molecular biology of FMRP: new insights into fragile X syndrome. Nat. Rev. Neurosci. 22, 209–222.
Rippin, I., Eldar-Finkelman, H., 2021. Mechanisms and therapeutic implications of gsk-3 in treating neurodegeneration. Cells 10, 1–22.
Rizk, M., Saker, Z., Harati, H., Fares, Y., Bahmad, H.F., Nabha, S., 2021. Deciphering the roles of glycogen synthase kinase 3 (GSK3) in the treatment of autism spectrum disorder and related syndromes. Mol. Biol. Rep. 48, 2669–2686.
Rorteau, J., Chevalier, F.P., Bonnet, S., Barthélemy, T., Lopez-Gaydon, A., Martin, L.S., Bechetoille, N., Lamartine, J., 2022. Maintenance of Chronological Aging Features in Culture of Normal Human Dermal Fibroblasts from Old Donors. Cells *11*.
Sala, C., Segal, M., 2014. Dendritic spines: the locus of structural and functional plasticity. Physiol. Rev. 94, 141–188.
Scarpulla, R.C., 2011. Metabolic control of mitochondrial biogenesis through the PGC-1 family regulatory network. Biochim. Biophys. Acta, Mol. Cell Res. 1813, 1269–1278.
Shah, K., Kazi, J.U., 2022. Phosphorylation-dependent regulation of WNT/Beta-catenin signaling. Front. Oncol. 12, 858782.
Shen, M., Wang, F., Li, M., Sah, N., Stockton, M.E., Tidei, J.J., Gao, Y., Korabelnikov, T., Kannan, S., Vevea, J.D., et al., 2019. Reduced mitochondrial fusion and huntingtin levels contribute to impaired dendritic maturation and behavioral deficits in Fmr1-mutant mice. Nat. Neurosci. 22, 386–400.
Shen, M., Sirois, C.L., Guo, Y., Li, M., Dong, Q., Méndez-Albelo, N.M., Gao, Y., Khullar, S., Kissel, L., Sandoval, S.O., et al., 2023. Species-specific FMRP regulation of RACK1 is critical for prenatal cortical development. Neuron 111, 3988–4005.e11.
Siegel, M., Beresford, C.A., Bunker, M., Verdi, M., Vishnevetsky, D., Karlsson, C., Teer, O., Stedman, A., Smith, K.A., 2014. Preliminary investigation of lithium for mood disorder symptoms in children and adolescents with autism spectrum disorder. J. Child Adolesc. Psychopharmacol. 24, 399–402.
Souder, D.C., Anderson, R.M., 2019. An expanding GSK3 network: implications for aging research. GeroScience 41, 369–382.
Souder, D.C., McGregor, E.R., Rhoads, T.W., Clark, J.P., Porter, T.J., Eliceiri, K., Moore, D.L., Puglielli, L., Anderson, R.M., 2023. Mitochondrial regulator PGC-1a in neuronal metabolism and brain aging.
Theeuwes, W.F., Gosker, H.R., Schols, A.M.W.J., Langen, R.C.J., Remels, A.H.V., 2020. Regulation of PGC-1α expression by a GSK-3β-TFEB signaling axis in skeletal muscle. Biochim. Biophys. Acta, Mol. Cell Res. 1867, 118610.
Thomas, C.I., Keine, C., Okayama, S., Satterfield, R., Musgrove, M., Guerrero-Given, D., Kamasawa, N., Young, S.M.J., 2019. Presynaptic mitochondria volume and abundance increase during development of a high-Fidelity synapse. J. Neurosci. 39, 7994–8012.
Toomey, C.E., Heywood, W.E., Evans, J.R., Lachica, J., Pressey, S.N., Foti, S.C., Al Shahrani, M., D'Sa, K., Hargreaves, I.P., Heales, S., et al., 2022. Mitochondrial dysfunction is a key pathological driver of early stage Parkinson's. Acta Neuropathol. Commun. 10, 134.
Trigo, D., Avelar, C., Fernandes, M., Sá, J., da Cruz, E., Silva, O., 2022. Mitochondria, energy, and metabolism in neuronal health and disease. FEBS Lett. 596, 1095–1110.
Ülgen, D.H., Ruigrok, S.R., Sandi, C., 2023. Powering the social brain: mitochondria in social behaviour. Curr. Opin. Neurobiol. 79, 102675.
Valenti, D., Vacca, R.A., 2023. Brain mitochondrial bioenergetics in genetic neurodevelopmental disorders: focus on down, rett and fragile X syndromes. Int. J. Mol. Sci. 24, 12488.
van Oostrum, M., Blok, T.M., Giandomenico, S.L., Tom Dieck, S., Tushev, G., Fürst, N., Langer, J.D., Schuman, E.M., 2023. The proteomic landscape of synaptic diversity across brain regions and cell types. Cell 186, 5411–5427.e23.
Vercellino, I., Sazanov, L.A., 2022. The assembly, regulation and function of the mitochondrial respiratory chain. Nat. Rev. Mol. Cell Biol. 23, 141–161.
Verdura, E., Pérez-Cano, L., Sabido-Vera, R., Guney, E., Hyvelin, J.-M., Durham, L., Gomez-Mancilla, B., 2021. Heterogeneity in Fragile X Syndrome Highlights the Need for Precision Medicine-Based Treatments. Front. Psychiatry *12*, 722378.
Wang, M., Liu, X., Hou, Y., Zhang, H., Kang, J., Wang, F., Zhao, Y., Chen, J., Liu, X., Wang, Y., et al., 2019. Decrease of GSK-3β Activity in the Anterior Cingulate Cortex of Shank3b (−/−) Mice Contributes to Synaptic and Social Deficiency. Front. Cell. Neurosci. 13, 447.
Wang, L., Li, J., Di, L.-J., 2022. Glycogen synthesis and beyond, a comprehensive review of GSK3 as a key regulator of metabolic pathways and a therapeutic target for treating metabolic diseases. Med. Res. Rev. 42, 946–982.
Weisz, E.D., Fenton, A.R., Jongens, T.A., 2024. PGC-1α integrates insulin signaling with mitochondrial physiology and behavior in a Drosophila model of Fragile X Syndrome. Npj Metab. Heal. Dis. 2, 2.
Westmark, P.R., Garrone, B., Ombrato, R., Milanese, C., Di Giorgio, F.P., Westmark, C.J., 2021. Testing Fmr1KO Phenotypes in Response to GSK3 Inhibitors: SB216763 versus AFC03127. Front. Mol. Neurosci. 14.
Xing, B., Li, Y.-C., Gao, W.-J., 2016. GSK3β Hyperactivity during an Early Critical Period Impairs Prefrontal Synaptic Plasticity and Induces Lasting Deficits in Spine Morphology and Working Memory. Neuropsychopharmacol. Off. Publ. Am. Coll. Neuropsychopharmacol. *41*, 3003–3015.
Xu, R., Hu, Q., Ma, Q., Liu, C., Wang, G., 2014. The protease Omi regulates mitochondrial biogenesis through the GSK3β/PGC-1α pathway. Cell Death Dis. *5* e1373.
Yang, K., Chen, Z., Gao, J., Shi, W., Li, L., Jiang, S., Hu, H., Liu, Z., Xu, D., Wu, L., 2017. The Key Roles of GSK-3β in Regulating Mitochondrial Activity. Cell. Physiol. Biochem. Int. J. Exp. Cell. Physiol. Biochem. Pharmacol. 44, 1445–1459.
Yuskaitis, C.J., Mines, M.A., King, M.K., Sweatt, J.D., Miller, C.A., Jope, R.S., 2010. Lithium ameliorates altered glycogen synthase kinase-3 and behavior in a mouse model of fragile X syndrome. Biochem. Pharmacol. 79, 632–646.
Zahedi, E., Sadr, S.S., Sanaeierad, A., Roghani, M., 2023. Valproate-induced murine autism spectrum disorder is associated with dysfunction of amygdala parvalbumin interneurons and downregulation of AMPK/SIRT1/PGC1α signaling. Metab. Brain Dis. *38*, 2093–2103.
Zhu, J., Rebecchi, M.J., Glass, P.S.A., Brink, P.R., Liu, L., 2013. Interactions of GSK-3β with mitochondrial permeability transition pore modulators during preconditioning: age-associated differences. J. Gerontol. A Biol. Sci. Med. Sci. 68, 395–403.